AMERICAN SOCIETY FOR MICROBIOLOGY | Journal of Virology

Human MicroRNA miR-532-5p Exhibits Antiviral Activity against West Nile Virus via Suppression of Host Genes SESTD1 and TAB3 Required for Virus Replication

Andrii Slonchak, Rory P. Shannon, Gabor Pali, Alexander A. Khromykh

Australian Infectious Diseases Research Centre, School of Chemistry and Molecular Biosciences, The University of Queensland, St Lucia, QLD, Australia

ABSTRACT

West Nile virus (WNV) is a mosquito-transmitted flavivirus that naturally circulates between mosquitos and birds but can also infect humans, causing severe neurological disease. The early host response to WNV infection in vertebrates primarily relies on the type I interferon pathway; however, recent studies suggest that microRNAs (miRNAs) may also play a notable role. In this study, we assessed the role of host miRNAs in response to WNV infection in human cells. We employed small RNA sequencing (RNA-seq) analysis to determine changes in the expression of host miRNAs in HEK293 cells infected with an Australian strain of WNV, Kunjin (WNV_{KUN}), and identified a number of host miRNAs differentially expressed in response to infection. Three of these miRNAs were confirmed to be significantly upregulated in infected cells by quantitative reverse transcription (qRT)-PCR and Northern blot analyses, and one of them, miR-532-5p, exhibited a significant antiviral effect against WNV_{KUN} infection. We have demonstrated that miR-532-5p targets and downregulates expression of the host genes SESTD1 and TAB3 in human cells. Small interfering RNA (siRNA) depletion studies showed that both SESTD1 and TAB3 were required for efficient WNV_{KUN} replication. We also demonstrated upregulation of mir-532-5p expression and a corresponding decrease in the expression of its targets, SESTD1 and TAB3, in the brains of WNV_{KUN} -infected mice. Our results show that upregulation of miR-532-5p and subsequent suppression of the SESTD1 and TAB3 genes represent a host antiviral response aimed at limiting WNV_{KUN} infection and highlight the important role of miRNAs in controlling RNA virus infections in mammalian hosts.

IMPORTANCE

West Nile virus (WNV) is a significant viral pathogen that poses a considerable threat to human health across the globe. There is no specific treatment or licensed vaccine available for WNV, and deeper insight into how the virus interacts with the host is required to facilitate their development. In this study, we addressed the role of host microRNAs (miRNAs) in antiviral response to WNV in human cells. We identified miR-532-5p as a novel antiviral miRNA and showed that it is upregulated in response to WNV infection and suppresses the expression of the host genes TAB3 and SESTD1 required for WNV replication. Our results show that upregulation of miR-532-5p and subsequent suppression of the SESTD1 and TAB3 genes represent an antiviral response aimed at limiting WNV infection and highlight the important role of miRNAs in controlling virus infections in mammalian hosts.

West Nile virus (WNV) is a mosquito-transmitted flavivirus associated with outbreaks of encephalitis in humans and horses around the world (1). The most significant WNV outbreaks have occurred in North America, where a highly pathogenic strain of WNV emerged in New York in 1999. This strain rapidly spread to all the states and by 2011 had infected an estimated 1.8 million people, causing close to 360,000 illnesses and ~1,300 deaths (2). The majority of these cases occurred between 2002 and 2007, followed by a period of relatively low activity in 2008 to 2011 (http://www.cdc.gov/westnile/statsmaps/). However, the infection rates in the United States increased again in 2012 to 2014, causing a total of 10,265 diagnosed infections and 502 deaths (http://www.cdc.gov/westnile/statsmaps/). In Australia, a relatively benign strain of WNV, Kunjin (WNV_{KUN}), has been circulating since the 1960s without causing noticeable outbreaks in either humans or horses (3). However, in 2011, a large outbreak of neurological disease in horses occurred in southern states, mainly in New South Wales (NSW), that was caused by an emerging pathogenic WNV_{KUN} strain that likely evolved from the less pathogenic WNV_{KUN} strains (4). As no specific treatment or approved vaccine is currently available for WNV, deeper insights into how the virus interacts with the host are essential for developing effective vaccines and/or antiviral drugs.

The early host response to WNV infection in vertebrates primarily relies on a type I interferon pathway (5). However, there is growing evidence suggesting that RNA-mediated pathways and, in particular, microRNA (miRNA)-related mechanisms play an important role in establishing and regulating the antiviral response against WNV infection (6, 7). miRNAs are 20- to 25-nucleotide (nt)-long RNAs that regulate gene expression by guiding the RNA-induced silencing complex (RISC) to partially complemen-

Received 12 October 2015 **Accepted** 7 December 2015

Accepted manuscript posted online 16 December 2015

Citation Slonchak A, Shannon RP, Pali G, Khromykh AA. 2016. Human microRNA miR-532-5p exhibits antiviral activity against West Nile virus via suppression of host genes SESTD1 and TAB3 required for virus replication. J Virol 90:2388–2402. doi:10.1128/JVI.02608-15.

Editor: M. S. Diamond

Address correspondence to Alexander Khromykh, a.khromykh@uq.edu.au.

tary sites within the 3′ untranslated regions (UTRs) of mRNAs, inducing their destabilization, degradation, or translational inhibition (8). miRNAs are involved in the regulation of diverse processes, including apoptosis, metabolism, cell fate determination, and host-pathogen interactions (9). miRNAs have been shown to regulate the host antiviral response by altering the expression of host genes required for virus replication and antiviral response (10–12) or by directly targeting viral genomes and/or transcripts (13–17).

Flaviviruses have been shown to induce significant changes in the expression of host miRNAs. Dengue virus (DENV) infection was shown to alter the expression of numerous miRNAs in mosquito (18) and human (19) cells. In particular, DENV strongly induced the expression of miR-146a in human monocytes, with significant benefit to virus replication (20). miR-146a inhibits the expression of tumor necrosis factor (TNF) receptor-associated factor 6 (TRAF6), a key molecule in the NF-κB signaling pathway (21). This inhibition of TRAF6 decreases the production of beta interferon (IFN-β) and facilitates DENV replication (20). Roles for other miRNAs in the antiviral response to DENV have also been demonstrated. For example, the expression of the host miRNA aae-miR-2940 was shown to restrict DENV replication in mosquitos by inhibiting expression of the methyltransferase gene *AaDnmt2* (22), whereas miR-281 was shown to enhance DENV replication in the mosquito gut (23). miR-30e (24), miR-223 (25), miR-548g-3p (26), and let-7c (27) were all shown to significantly inhibit DENV-2 replication in human cells by altering the expression of various host genes. In addition, roles of a number of mammalian miRNAs in response to Japanese encephalitis virus (JEV) infection have also been reported. miR-15b and miR-155 were shown to induce an inflammatory response in JEV-infected microglial cells via suppression of RNF125 (28) and SHIP1 (29), respectively, whereas miR-146a was shown to inhibit the immune response against JEV by suppressing the JAK/STAT pathway in mouse monocytes (30). WNV infection has been shown to alter the expression of the inflammatory miRNAs miR-196a, miR-202-3p, miR-449c, and miR125a-3p in the mouse brain (31). The downregulation of these miRNAs following infection was shown to contribute to WNV pathogenesis by promoting inflammation and neuronal cell death (31). Similarly, miR-6124 was found to be substantially upregulated in response to WNV infection in the neuronal epithelioma SK-N-MC cell line (6). miR-6124 has a proapoptotic role, repressing the expression of the antiapoptotic proteins CTCF and ECOP, which are important for WNV pathogenesis (6).

Previously, we demonstrated that the host response against WNV_{KUN} in mosquito cells involves the downregulation of the miRNA aae-miR-2940-5p, which is required for viral replication (32). Increased miR-2940-5p expression inhibited virus replication via suppression of a host metalloprotease, m41 FtsH, required for virus replication (32). In the current study, we investigated the role of host miRNAs in WNV_{KUN} infection of human cells. We show that expression of miR-532-5p is upregulated in response to WNV_{KUN} infection, which results in the suppression of the SESTD1 (SEC14 and spectrin domains 1) and TAB3 genes required for virus replication. Thus, we conclude that upregulation of miR-532-5p with subsequent suppression of the SESTD1 and TAB3 genes represents a host response aimed at limiting WNV_{KUN} infection.

MATERIALS AND METHODS

Cell culture and infection. Human embryonic kidney cells (HEK293), green monkey kidney epithelial cells (Vero), and baby hamster kidney fibroblasts (BHK-21) were grown in high-glucose Dulbecco modified Eagle's medium (DMEM) supplemented with 10% fetal bovine serum (FBS) (Bovogen, Australia) and 2 mM L-glutamine. The cells were maintained in a humidified atmosphere of air and 5% CO_2 at 37°C.

Passage 0 (P0) WNV_{KUN} was generated from an FLSDX infectious cDNA clone as described previously (33) and amplified in Vero cells to produce high-titer passage 1 (P1) virus. Vero cells were infected with P0 WNV_{KUN} at a multiplicity of infection (MOI) of 0.1, and culture fluid was collected at 3 days postinfection (dpi). Virus titers were determined by plaque assay on BHK-21 cells. The resulting P1 virus stock was then used in all infection experiments.

All infections were carried out by incubation of cells with a small volume of medium (45 μl/cm^2 of growth area) containing virus at the indicated MOI; then, the inoculum was removed, the cells were washed twice, and fresh medium was added. Infections were performed, and the infected cells were maintained in DMEM supplemented with 2% FBS. All cell culture reagents were from Gibco, Life Technologies Inc. (USA) unless otherwise specified.

Plaque assay for WNV_{KUN} titers. Serial dilutions of culture fluids were prepared, and 200 μl of each dilution was used to infect BHK-21 cells grown in 6-well plates, followed by incubation for 2 h and overlaying with DMEM containing 0.5% low-melting-point agarose (Rio-Rad, USA) and 2% FBS. At 72 h postinfection, cells were fixed with 4% phosphate-buffered saline (PBS)-buffered formaldehyde, stained with crystal violet, and washed with water. Plaques were then counted, and titers were calculated based on the dilution factor.

RNA isolation. Total RNA was isolated from HEK293 cells using TRI Reagent (Sigma-Aldrich, USA). Enriched small-RNA fractions were isolated using a mirVana miRNA isolation kit (Ambion, USA). All manipulations were performed according to the manufacturers' instructions.

MicroRNA sequencing. Enriched small-RNA fractions isolated from infected and uninfected HEK293 cells were used to construct libraries of mature miRNAs and pre-miRNAs. A mature miRNA library was generated using a Truseq small-RNA preparation kit (Illumina, USA) according to Illumina's sample preparation guide. The purified cDNA library was used for cluster generation on Illumina's Cluster Station and then sequenced on an Illumina GAIIx following the vendor's instructions. Raw sequencing reads (40 nt) were obtained using Illumina's Sequencing Control Studio software version 2.8 (SCS v2.8) following real-time sequencing image analysis and base calling with Illumina's Real-Time Analysis version 1.8.70 (RTA v1.8.70). A proprietary pipeline script, ACGT101-miR v4.2 (LC Sciences, USA), was used to trim the adaptor sequences, remove various unmappable sequencing reads, and map the remaining unique reads with the reference database files of mature miRNAs (ftp://mirbase.org/pub/mirbase/CURRENT/). The RNA library for pre-miRNA sequencing was prepared using an mRNA-Seq Sample Prep kit (Illumina, USA), and sequencing was conducted on an Illumina HiSeq 2000 instrument according to the manufacturer's protocol. The 3′ adaptor for sequencing was removed from the raw reads, and reads with a length of less than 10 nt were excluded. The remaining reads were aligned with human pre-miRNAs (ftp://mirbase.org/pub/mirbase/CURRENT/) using Bowtie v1.0.0. The number of read copies from each sample was tracked during mapping of mature miRNAs and pre-miRNAs and normalized for comparison. The ACGT101-miR v4.2 script (LC Sciences, USA) was then used to perform the differential-expression analysis. Normalization of sequence counts in each sample (or data set) was achieved by dividing the read counts by a library size parameter of the corresponding sample. The library size parameter was a median value of the ratio between the counts in a specific sample and a pseudo-reference sample. A count number in the pseudo-reference sample was the geometric mean count across all samples. Library preparations, sequencing, and bioinformatic analysis were performed by LC Sciences, LLC (Houston, TX, USA).

Quantitative RT-PCR. The stem-loop reverse transcription (SL-RT)-PCR method (34) was used to determine the expression of miRNAs in infected and uninfected HEK293 cells. RT reactions were performed on enriched small-RNA fractions using a TaqMan MicroRNA reverse transcription kit (Applied Biosystems, USA), following the multiplex RT protocol. RT primers (Table 1) annealed to the stem-loop conformation by heating to 100°C, followed by gradual cooling to room temperature, were used for the RT reaction. The 40-μl reaction mixture containing 2 μg small RNA, 400 units of Multiscribe RT enzyme, 10 units of RNase inhibitor, 2 mM deoxynucleoside triphosphates (dNTPs), and 4 pmol of each RT primer was incubated at 16°C for 30 min and then at 42°C for 30 min and 85°C for 5 min. The synthesized cDNA was diluted 10-fold, and 5 μl of the diluted cDNA was used for quantitative RT-PCR (qRT-PCR), which was carried out using the common reverse primer and miRNA-specific forward primers (Table 1).

The cDNA for quantitative detection of mRNA levels was synthesized with a qScript cDNA synthesis kit (Quanta Biosciences, USA) using total cell RNA as a template. The RT reaction was performed according to the manufacturer's instructions. The resulting cDNA was diluted 1:50, and 3 μl of the diluted cDNA was used for quantitative PCR (qPCR) with the primers listed in Table 2.

All qRT-PCRs were performed on a ViiA7 Real Time PCR instrument (Applied Biosystems, USA) using SYBR green PCR master mix (Applied Biosystems, USA) in a reaction volume of 20 μl with 10 pmol of each primer. All reactions except amplification of miR-532-5p and miR-1307-3p were performed using the following cycling conditions: 95°C for 10 min and 40 cycles of 95°C for 15 s and 60°C for 1 min, followed by melting-curve analysis. The annealing/extension temperature for amplification of miR-532-5p and miR-1307-3p was 65°C.

Gene expression analysis was performed by the $\Delta\Delta C_T$ method (35) using ViiA7 software (Applied Biosystems, USA). Expression of miRNAs was normalized to the miR-30e-5p level, and expression of mRNAs was normalized to the TATA-binding protein (TBP) mRNA level and compared to mock-infected samples. For each experiment, RNA from 3 biological replicates was used, RT reactions were performed in triplicate for each RNA sample, and PCR amplification of each cDNA sample was done in triplicate. No-RT controls were included for each RNA sample, and no-template controls were included for each primer pair.

Northern blotting. Northern blot analysis of miRNA expression was performed as described previously (32), using 5 μg of enriched small-RNA fraction. The DNA oligonucleotides used as probes are listed in Table 1.

Transfection of miRNA mimics and inhibitors. To assess the effect of miRNAs on WNV replication and expression of potential target genes, HEK293 cells were transfected with the synthetic miRNA mimics and inhibitors listed in Table 3. MicroRNA-specific mimics and inhibitors, a nonspecific miRNA mimic and inhibitor, and a 6-carboxyfluorescein (FAM)-labeled nonspecific miRNA mimic and inhibitor were synthetized by Shanghai GenePharma Co (China) and Dharmacon (USA). HEK293 cells were transfected with miRNA mimics or inhibitor in suspension using Lipofectamine 2000 transfection reagent (Invitrogen, USA). For each transfection, 60 pmol of miRNA mimic or 120 pmol of miRNA inhibitor was diluted in 300 μl Opti-MEM reduced-serum medium (Gibco, USA), mixed with 300 μl of the same medium containing 12.5 μl Lipofectamine 2000, and incubated at room temperature for 30 min to allow complex formation. Then, 1 ml of cell suspension containing 5×10^5 HEK293 cells in DMEM supplemented with 10% FBS was added to the complex, mixed, and transferred to the wells of 6-well plates.

Computational prediction of miRNA targets. The potential target sites for host miRNAs were predicted in the WNV genome (GenBank accession number AY274504) using RNAhybrid software (36). miRNA/target duplexes with a minimum fold energy of greater than or equal to −27 kcal/mol and a maximum external bulge size of 5 nt were considered potential interactions.

The potential targets for miR-532 in the human transcriptome were

TABLE 1 Oligonucleotides used as primers for miRNA-specific qRT-PCR detection and probes used for miRNA detection by Northern blotting

miRNA name	miRNA sequence[a] (5′–3′)	miRBase accession no.	SL-RT primer sequence (5′–3′)	Forward PCR primer sequence (5′–3′)	Northern blot probe sequence (5′–3′)
hsa-miR-1271-5p	CUUGGCACCUAGCAAGCACUCA	MIMAT0005796	GTCGTATCCAGTGCAGGGTCCGAGGTA TTCGCACTGGATACGACTGAGTG	TGGAGACTTCGCACCTAGCAAG	ACTAGACTGTGAGCTCCTCGA
hsa-miR-1307-5p	UCGACCGGACCUCGACCGGCU	MIMAT0022727	GTCGTATCCAGTGCAGGGTCCGAGGTA TTCGCACTGGATACGACAGCCGG	AGTTCTTTCGACGGGACCTCGA	AGCCGGTCGAGGTCCGGTCGA
hsa-miR-151b	UCGAGGAGCUCACAGUCUAGU	MIMAT0010214	GTCGTATCCAGTGCAGGGTCCGAGGTA TTCGCACTGGATACGACACTAGA	TGGTTTCTTCGAGGAGGTCACAG	ACTAGACTGTGAGCTCCTCGA
hsa-miR-22-3p	AAGCUGCCAGUUGAAGAACUGU	MIMAT0000077	GTCGTATCCAGTGCAGGGTCCGAGGTA TTCGCACTGGATACGACACAGTT	AGGAGGAAGCUGCCAGUUGAAG	ACAGTTCTTCAACTGGCAGCTT
hsa-miR-24-3p	UGGCUCAGUUCAGCAGGAAC	MIMAT0000080	GTCGTATCCAGTGCAGGGTCCGAGGTA TTCGCACTGGATACGACGTTCCT	AGGAGGGTTGGTTCAGTTCAGC	GTTCCTGCTGAACTGAGCCA
hsa-miR-25-3p	CAUUGCACUUGUCUCGGUCUGA	MIMAT0000081	GTCGTATCCAGTGCAGGGTCCGAGGTA TTCGCACTGGATACGACTCAGAC	AGCCTCCATTCCACTTGTCTCG	TCAGACCGAGACAAGTGCAATG
hsa-miR-30e-3p	CUUUCAGUCGGAUGUUUACAGC	MIMAT0000693	GTCGTATCCAGTGCAGGGTCCGAGGTA TTCGCACTGGATACGACGCTGTA	GGTCGGCTTTCAGTCGGATGTT	GCTGTAAACATCCGACTGAAAG
hsa-miR-532-5p	CAUGCCUUGAGUGUAGGACCGU	MIMAT0002888	GTCGTATCCAGTGCAGGGTCCGAGGTA TTCGCACTGGATACGACACGGTC	TGGGTCCTTGCCTTGAGTGTAG	ACGGTCCTACACTCAAGGCATG

[a] Universal miRNA reverse PCR primer, 5′-GGTCGGCTTTCAGTCGGATGTT-3′.

TABLE 2 Sequences of primers used for mRNA qRT-PCR

Gene symbol	GenBank accession no.	Forward primer (5′–3′)	Reverse primer (5′–3′)
GAPDH	NM_002046	GAAGGCTGGGGCTCATTTGC	TAAGCAGTTGGTGGTGCAGG
Zfhx3	NM_001164766	TGCTACTACCACTGCGTTCTG	CAATGGCTTCTTCTGGGTCCG
SESTD1	NM_178123	AGACTCACATCAGATTGGGCG	TGCCATAGTCATAAGTGCTCTGT
TAB3	NM_152787	GCAAGGATGGAGAGGTTAGCA	GTCATTTCCTCAGGCGTAGGG
DHX9	NM_001357	ACAAAGAAGAAGGAAGGAGAGACA	GACCAAGGAACCACACCCAC
CPEB3	NM_001178137	TGTCAAAATGGGGAACGAGTAGA	TGTCAAAATGGGGAACGAGTAGA
TRAPPC2P1	NM_014563	GCTTGGTTCCTTGTACGCAGA	ATATGGCTCCTCGGGTTCTTC
METTL20	NM_001135864	CCAAGCCTCTAAGCCTCACAG	AACCGGAACCTCTGACTCGGA
ZNF536	NM_014717	AGTGACCAAAACCTTGCTTGG	TCGCTTCTTCCATCCCTTGAG
SMAD2	NM_001003652	GAAGGAACAAAAGGTCCCGGA	TGAATGGCAAGATGGACGACA
FAM116A	NM_152678	GCTTGGATGTTTTCCAGAGACATT	GGCTTTCTGGGTCAGGAGTG
RASSF5	NM_182665	GGGACACGAAACCGCAGAG	CCGTCCTTGTGTATCCGCTT
GBP1	NM_002053	CCCAGCCCTACAACTTCGG	ATGTCCAGGCTGTTCCCTTG
ARMC8	NM_014154	GGTACTTGAGCGGTGTCCAG	ATTCCTGGTCCGAAAGGACG
CPNE1	NM_152926	CCGACGGCCATTTTGTGAAG	GCTGAACGGGGACTGAGAAA
WNV NS4A region	AY274504	TTGAGTGTGATGACCATGGGAG	TAGCTGGTTGTCTGTCTGCG

predicted using the TargetScanHuman (37), PicTar (38), RNA22 (39), DIANA-MicroT (40), microRNA.org (41), miRDB (42), TargetMiner (43), and Tarbase (44) algorithms. The lists of genes generated by the programs were cross-checked, and targets predicted by at least 5 algorithms were selected for further analysis.

MicroRNA sensor constructs and luciferase reporter assay. Luciferase reporter plasmids were constructed by cloning double-stranded synthetic oligonucleotides (Table 4) containing miRNA target sequences flanked by PmeI and XbaI sites into the PmeI/XbaI-digested pmirGLO Dual-Luciferase miRNA Target Expression Vector (Promega, USA). Plasmids were transformed into chemically competent *Escherichia coli* XL10-Gold cells (Agilent Technologies, USA). Positive transformants were selected by colony PCR with primers specific to the pmirGLO vector (pmirGLO F, 5′-TCGTGGACGAGGTGCCTAAA-3′; pmiRGLO R, 5′-TTAGCAGCCGGATCAGCTTG-3′) and used to isolate the plasmids from 5 ml of overnight culture using a Wizard SV Miniprep kit (Promega, USA). The extracted plasmid DNA was then subjected to Sanger sequencing to confirm the sequences of the inserts. Sequencing was performed by the Australian Genome Research Facility (Brisbane, Australia) using an AB3730xl DNA analyzer (Applied Biosystems, USA). Plasmid DNA for transfection was isolated from 200 ml of overnight culture using an EndoFree Maxi Plasmid Isolation kit (Qiagen, USA).

To assess the effect of miRNA on expression of the luciferase gene containing the corresponding target site, the reporter constructs were cotransfected into HEK293 cells, together with miR-532-5p-specific or control miRNA mimic. For each well of a 96-well plate, 10 pmol of miRNA mimic and 100 ng of plasmid were incubated with 0.5 μl Lipofectamine 2000 (Invitrogen, USA) in 60 μl Opti-MEM reduced-serum medium (Gibco, USA) for 30 min; 4.5×10^4 cells were then added in a 40-μl volume of DMEM supplemented with 10% fetal calf serum (FCS). At 24 h posttransfection (hpt), the culture medium was replaced with 25 μl PBS, and luciferase expression was determined using the Dual-Glo luciferase assay system (Promega, USA) and a Lucy 2 microplate luminometer (Anthos Labtec Instruments, United Kingdom). Measurements were performed according to the manufacturer's protocol with a 10-s signal integration time for each luciferase, and the relative luciferase expression was calculated as a ratio of firefly to *Renilla* luciferase activity.

RNAi knockdown. HEK293 cells were transfected with a mixture of 3 individual Stealth RNA interference (RNAi) small interfering RNAs (siRNAs) (20 μM each) to SESTD1 (Invitrogen, USA), siGenome Pool siRNA to TAB3 (Dharmacon, USA), or corresponding negative-control siRNAs (Dharmacon, USA) using Lipofectamine 2000 transfection reagent (Invitrogen). For each transfection, 120 pmol of siRNA was diluted in 300 μl Opti-MEM reduced-serum medium (Gibco, USA), mixed with 300 μl of the same medium containing 12.5 μl Lipofectamine 2000, and incubated at room temperature for 30 min. Then, 1 ml of the cell suspension containing 5×10^5 HEK293 cells in DMEM supplemented with 10% FBS was added to the complex, mixed, and transferred to the wells of 6-well plates.

Western blotting. HEK293 cells cultured in 6-well plates were washed with 1 ml of PBS per well and lysed in RIPA buffer (200 μl/well) supplemented with Complete proteinase inhibitor cocktail (Roche). The lysates were centrifuged at 16,000 × *g* for 5 min at 4°C, the supernatants were collected, and protein concentrations were determined by Bio-Rad Protein Assay (Bio-Rad, USA). To digest contaminating chromosomal DNA, 1 μl of Benzonase nuclease (Sigma, USA) was added to each sample and incubated for 20 min at room temperature. Samples containing 25 μg of protein were mixed with Novex NuPAGE LDS sample buffer (Life Technologies, USA) and Novex Bolt sample reducing agent (Life Technologies, USA) and denatured at 95°C for 5 min. Samples were loaded onto Novex Bolt 4 to 12% Bis-Tris gels (Life Technologies, USA), and electrophoresis was performed at 200 V for 35 min in Novex Bolt MES-SDS running buffer (Life Technologies, USA). Proteins were then electroblotted to Amersham Protran Premium 0.45-μm nitrocellulose blotting membranes

TABLE 3 Sequences of miRNA mimics and inhibitors

	Sequence (5′–3′)		
	Mimic		
miRNA name	Sense strand	Antisense strand	Inhibitor
miR-1271	UUGGCACCUAGCAAGCACUCA	UGAGUGCUUGCUAGGUGCCAAGdTdT	ACTAGACTGTGAGCTCCTCGA
miR-532	CAUGCCUUGAGUGUAGGACCGU	ACGGUCCUACACUCAAGGCAUGdTdT	ACGGTCCTACACTCAAGGCATG
miR-1307	ACTCGGCGTGGCGTCGGTCGTGG	CCACGACCGACGCCACGCCGAGUdTdT	AGCCGGTCGAGGTCCGGTCGA
Nonspecific	GAACUGUAUGUCGGAAUAGGTT	CCUAUUCCGACAUACAGUUCdTdT	CCUAUUCCGACAUACAGUUC

TABLE 4 Sequences of the synthetic inserts for reporter constructs

Name	Sequence (5′–3′)	
	Sense strand	Antisense strand
WNV putative target 1	AAACTAGCGGCCGCCATGGTCCATCCACGCTGGAG GAGAGTGGT	CTAGACCACTCTCCTCCAGCGTGGATGGACCATGGC GGCCGCTAGTTT
WNV putative target 2	AAACTAGCGGCCGCCCGAGCCTGGAACTCAGGGT ATGAT	CTAGATCATACCCTGAGTTCCAGGCTCGGGCGGCCGCT AGTTT
WNV scrambled target	AAACTAGCGGCCGCGCCCCTACGAGCTAAGTGTACAT	CTAGATGTACACTTAGCTCGTAGGGGCGCGGCCGCTAGTTT
miR-532-5p positive control	AAACTAGCGGCCGCACGGTCCTACACTCAAGGCATGT	CTAGACATGCCTTGAGTGTAGGACCGTGCGGCCGCTAGTTT
TAB3 target	TAGAGCTCATTTGTAGCAGTCAGGAACTAGGCATA TCATGCCTATTTGTTCTGACAGTATAAACAAA AAGAATATAAGGCATAGAAGAATTGTCCAATC ATTTTGAGATGAAATTGTACAAAGGCATTT TAAAAGTCTAGAAT	ATTCTAGACTTTTAAAATGCCTTTGTACAATTTCATCTCAA AATGATTGGACAATTCTTCTATGCCTTATATTCT TTTTGTTTATACTGTCAGAACAAATAGGCATGAT ATGCCTAGTTCCTGACTGCTACAAATGAGCTCTA
TAB3 scrambled	TAGAGCTCTTAAGTATAGGAAAATTCCAAACACAC TTACAATTAATCTGTTATAGGGTTATTTGATGG GGAATATACATAACATGAGTTAGTATA GATAAAAGCATATTAAGACCACGGCGA CTTCGAAAAGTCTAGAAT	ATTCTAGACTTTTCGAAGTCGCCGTGGTCTTAATATGC TTTTATCTATACTAACTCATGTTATGTATATTCCCC ATCAAATAACCCTATAACAGATTAATTGTAAGTGTGT TTGGAATTTTCCTATACTTAAGAGCTCTA
SESTD1 target	TAGAGCTCCTCTTTACATGTTAACACCTTGCTACT ACCAAGGCATAATTACTTAACATTTTGTCTTT AGGGGAGGAGGGCTGAGGAAGAAGGCATACATA ATTACTTCAGTGTTCCTACTGAGAAGTCC ATTTTTAAGGCATCAAAGGTGAATTCTAGATT	AATCTAGAATTCACCTTTGATGCCTTAAAAATGGACTTCTC AGTAGGAACACTGAAGTAATTATGTATGCCTTCTTCC TCAGCCCTCCTCCCCTAAAGACAAAATGTTAAGTA ATTATGCCTTGGTAGTAGCAAGGTGTTAACATGT AAAGAGGAGCTCTA
SESTD1 scrambled	TAGAGCTCTCTCTAGCGTTCTATTCTCGCTTGTAT TCTCTCGCACGGACAAGTTAATAGAAATAGGT GCGAAGTTATGTATGTGAAGAATTACTTGGCA GAGAAACACAATAAGTCGAGCACTGTTGAATATA CGAGCTATAGACTCTTCTATTCTAGATT	AATCTAGAATAGAAGAGTCTATAGCTCGTATATTCAACAGT GCTCGACTTATTGTGTTTCTCTGCCAAGTAATTCTT CACATACATAACTTCGCACCTATTTCTATTAACT TGTCCGTGCGAGAGAATACAAGCGAGAATAGAACG CTAGAGAGAGCTCTA

(GE Healthcare Life Science, USA) at 100 V for 1 h in Tris-glycine transfer buffer (25 mM Tris, 192 mM glycine, 0.1% SDS, 20% methanol) using a Mini Trans-Blot electrophoretic transfer cell (Bio-Rad, USA). The membranes were blocked for 1 h in 3% nonfat milk in PBS, incubated with primary antibodies (Abs) overnight at 4°C, and then washed 4 times for 5 min each time in phosphate-buffered saline containing 0.05% Tween 20 (PBST) and incubated with secondary antibodies for 1 h at room temperature. Then, the antibodies were removed and washing was repeated. Antibodies were diluted in 3% nonfat milk in PBS as follows: anti-TAB3 rabbit polyclonal Ab (Sigma, USA), 1:2,000; anti-SESTD1 rabbit polyclonal Ab (Sigma, USA), 1:500; anti-GAPDH (glyceraldehyde-3-phosphate dehydrogenase) mouse monoclonal Ab (Sigma, USA), 1:10,000; anti-WNV E protein mouse monoclonal Ab 3.91D (a gift from Roy Hall [45]), 1:200; and anti-mouse and anti-rabbit IgG horseradish peroxidase (HRP)-linked Abs (Cell Signaling, USA), 1:5,000. Chemiluminescent signal detection was performed using Pierce ECL Plus Western blotting substrate (Thermo Scientific, USA) according to the manufacturer's instructions, followed by exposure to SuperRX Fuji Medical X-Ray Film (Fujifilm, Japan). The films were developed using an XP-9000 X-ray film automatic processor (DLC Pty Ltd., Australia) and scanned. Densitometry was performed using ImageJ software (NIH).

For detection of multiple proteins on the same membrane, membranes were stripped and reprobed. A mild stripping protocol was used. The membranes were washed two times for 10 min each time with mild stripping buffer (1.5% glycine, 0.1% SDS, 1% Tween 20) and then two times for 10 min each time in PBS and two times for 5 min each time with PBST.

Infection of mice and isolation of total mouse brain RNA. Groups of five 21-day-old Swiss outbred mice (CD-1) were injected intraperitoneally with 10,000 PFU of WNV_{KUN} NSW2011 in DMEM. As a control, three mice were injected with DMEM. The mice were monitored three times per day for 14 days for clinical symptoms of WNV infection (ruffled fur, antisocial behavior, paralysis, and hunched posture). Mice that showed symptoms of encephalitis were euthanized, and their brains were collected. Total brains were homogenized in 1 ml of cold diethyl pyrocarbonate (DEPC)-PBS using a TissueLyser II homogenizer (Qiagen, USA). The homogenate (250 μl) was used for RNA isolation with Tri Reagent LS (Sigma-Aldrich, USA) according to the manufacturer's protocol. All infection experiments were conducted within a physical containment level 2 (PC2) animal house facility. All animal procedures had received prior approval from the University of Queensland Animal Ethics Committee in accordance with the guidelines for animal experimentation as set out by the National Health and Medical Research Council, Australia.

Statistic analysis. The results of qRT-PCR (Fig. 1B; see Fig. 4A) and luciferase reporter assays (see Fig. 3B and 5B) were analyzed by Student's *t* test. Virus growth kinetics (Fig. 2; see Fig. 6C and D) were analyzed by two-way analysis of variance (ANOVA) on data linearized by taking natural logarithms of titers (46). Bonferroni correction was applied for multiple comparisons. Analysis was performed using Prism 6 software (GraphPad Software, USA).

RESULTS

MicroRNAs miR-1271-5p, miR-532-5p, and miR-1307-3p are differentially expressed in WNV_{KUN}-infected cells. In order to identify the miRNAs involved in the host response to WNV_{KUN} infection, we examined the expression of mature miRNAs and their precursors (pre-miRNAs) in infected and uninfected HEK293 cells. Mature miRNAs are the primary effector molecules in the miRNA pathways, regulating the expression of target genes by guiding RISC to complementary mRNAs. As miRNAs bind to target mRNAs stoichiometrically, the level of mature miRNAs in cells determines the degree of their regulatory effect on the targeted mRNAs. Therefore, the levels of mature miRNAs are most

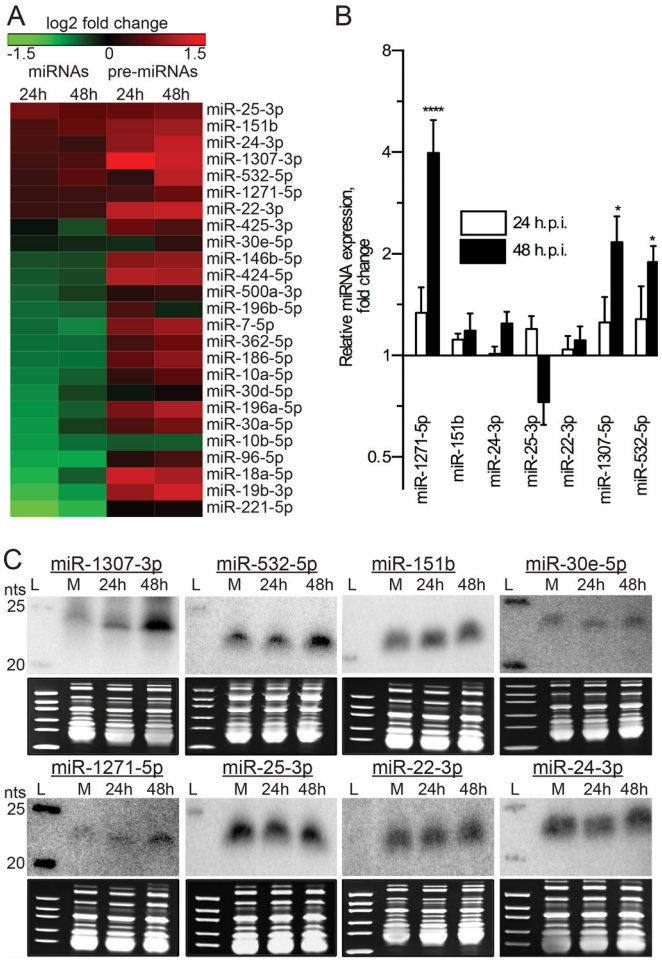

FIG 1 WNV_{KUN} infection alters expression of host miRNAs in HEK293 cells. (A) Heat map representation of miRNA and pre-miRNA expression in HEK293 cells at 24 h and 48 h after WNV_{KUN} infection. miRNAs are ranked in descending order based on the fold change in mature miRNA levels in infected cells compared to the uninfected control. Only miRNAs representing more than 0.1% of the total mappable miRNA reads are shown. (B) Quantitative RT-PCR analysis of miRNA expression in HEK293 cells infected with WNV_{KUN} expressed as relative fold changes compared to mock infection. The values represent the means of 3 biological replicates, with the error bars showing standard deviations. *, $P < 0.05$; ****, $P < 0.0001$. (C) Northern blot analysis of miRNA expression in HEK293 cells before (M) and at 24 h and 48 h after WNV_{KUN} infection. Ethidium bromide-stained tRNA (upper gels) and 5S rRNA (lower gels) served as RNA loading controls and indicators of RNA integrity in the samples. L, molecular weight ladder.

commonly used as indications of the host responses to various conditions, including virus infections. However, WNV_{KUN} infection was shown previously to inhibit Dicer activity, involved in miRNA processing (47). This is likely to result in general and nonspecific alterations in the levels of processed mature miRNAs, which makes identification of miRNAs specifically modulated by infection less informative if only the levels of mature miRNAs are measured. Therefore, in addition to mature miRNAs, we also determined the expression levels of pre-miRNAs in WNV_{KUN}-infected cells. Unlike mature miRNAs, which are usually very stable, pre-miRNAs have very fast turnover (48) and thus provide a more direct indication of the changes in transcriptional activation of the host miRNA genes in response to infection. Only miRNAs that showed comparable responses, i.e., up- or downregulation, in both mature miRNAs and pre-miRNAs were considered to be potentially involved in the host response to infection in this study.

To examine the effect of WNV_{KUN} infection on miRNA expression, HEK293 cells were infected with WNV_{KUN} at an MOI of 1 PFU/cell, RNA was collected at 24 and 48 h postinfection (hpi), and the expression of miRNAs and their precursors was determined by Illumina sequencing (transcriptome sequencing [RNA-seq]). RNA isolated from uninfected cells was used as a control. We observed differential expression of multiple miRNAs in infected cells compared to the uninfected control at 24 and 48 hpi. Taking into account that only miRNAs contributing at least 0.1% of the total miRNA pool are likely to exhibit biological activity (49), only differentially expressed miRNAs represented by more than 1,000 reads per million in the RNA-seq results were considered for further analysis. As a result, only 7 upregulated and 17 downregulated miRNAs in WNV_{KUN}-infected cells satisfied our criteria (Fig. 1A).

Analysis of the expression of corresponding pre-miRNAs revealed that 23 of these 24 pre-miRNAs (the exception was miR-10a) were actually expressed at higher levels in infected cells despite the fact that expression of 17 of their processed miRNA products was downregulated (Fig. 1A). This inconsistency between the expression of mature miRNAs and their precursors indicates that WNV_{KUN} infection may either supress pre-miRNA processing into mature miRNAs or enhance degradation of mature miRNAs. The former is likely explained by the inhibition of Dicer in WNV_{KUN}-infected cells, while the latter may involve an as-yet-unidentified mechanism. We therefore focused on analysis of 7 miRNAs that we upregulated at the levels of both mature miRNA and pre-miRNA, i.e., miR-25-3p, miR-151b, miR-24-3p, miR-1307-3p, miR-532-5p, miR-1271-5p, and miR-22-3p (Fig. 1A).

In order to validate the results of RNA-seq analysis, qRT-PCR analysis was used to determine the levels of these 7 miRNAs in WNV_{KUN}-infected and uninfected HEK293 cells. The expression of each individual miRNA was determined at 24 and 48 hpi (Fig. 1B), with normalization to miR-30e, whose expression was not significantly altered as a result of infection (Fig. 1A and C). The results demonstrated that miR-1271-5p was the most upregulated miRNA, with a 4-fold increase in expression in infected cells at 48 hpi, while expression of miR-1307-3p and miR-532-5p was upregulated approximately 2-fold (Fig. 1B). The observed differences in miR-1271-5p, miR-1307-3p, and miR-532-5p expression between WNV_{KUN}-infected and mock-infected cells were statistically significant. The expression of miR-151b, miR-24-3p, miR-22-3p, and miR-25-3p was not significantly altered upon infection.

To further validate the results of RNA-seq and qRT-PCR analyses, small-RNA fractions from WNV_{KUN}-infected and uninfected HEK293 cells were subjected to Northern blot analysis using radioactive probes complementary to the corresponding miRNA sequences. The results revealed that miR-1307-3p, miR-1271-5p, and miR-532-5p were indeed upregulated in infected cells compared to mock-infected cells, with a notable increase at 48 hpi (Fig. 1C). Consistent with the qRT-PCR results, Northern blot analysis did not identify notable changes in the expression of miR-151b, miR-25-3p, miR-22-3p, and miR-24-3p (Fig. 1C).

The combined results of RNA-seq, qRT-PCR, and Northern blot analyses of miRNA expression showed that 3 host miRNAs,

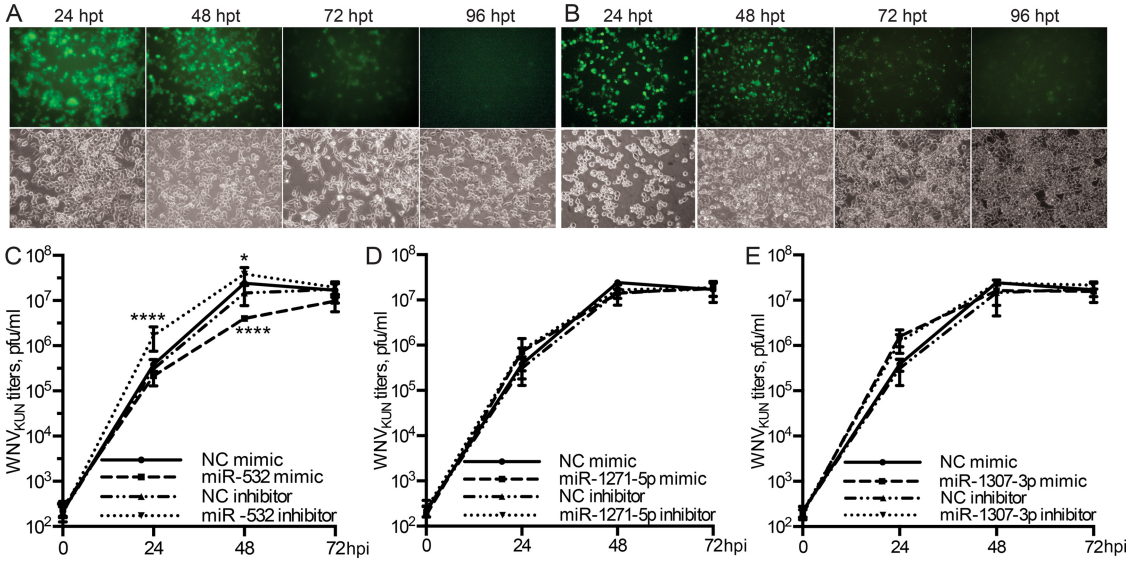

FIG 2 Effects of miRNA mimics and inhibitors on WNV_{KUN} replication. (A and B) Transfections with FAM-labeled miRNA mimic (A) and inhibitor (B) were performed to estimate transfection efficiency and to monitor for the presence of RNA oligonucleotides in the cells in time course experiments. (C to E) HEK293 cells were transfected with synthetic mimics or inhibitors specific to miR-532-5p (C), mir-1271-5p (D), or miR-1307-3p (E). Cells transfected with nonspecific mimic or inhibitor were used as a negative control (NC). At 24 h posttransfection, the cells were infected with WNV_{KUN} at an MOI of 1, and virus titers in the culture fluids at the indicated times postinfection (hpi) were determined by plaque assay on BHK-21 cells. Titers are shown as means of biological replicates, with the error bars showing standard deviations. *, $P < 0.05$; ****, $P < 0.0001$.

miR-1271-5p, miR-532-5p, and miR-1307-3p, were significantly upregulated in response to infection. Therefore, these miRNAs were selected for further analysis of their potential roles in WNV_{KUN} infection.

MicroRNA miR-532-5p inhibits WNV_{KUN} replication. In order to examine the effects of miR-1271-5p, miR-532-5p, and miR-1307-3p on WNV_{KUN} replication, miRNA gain-of-function and loss-of-function experiments were performed. HEK293 cells were transfected with either an miRNA-specific or a nonspecific mimic or inhibitor and then infected with WNV_{KUN} at an MOI of 1. The detection of FAM-labeled nonspecific mimics and inhibitors at each of these time points showed that approximately 90% of the cells were transfected with miRNA mimics and inhibitors and that these were retained at high levels at 24 and 48 hpt (Fig. 2A and B). At 72 hpt, intracellular levels of transfected mimics and inhibitors started to decrease and became almost undetectable at 96 hpt (Fig. 2A and B). The viral titers in culture fluids from cells transfected with the control mimic or inhibitor increased before reaching a peak of 2.75×10^7 PFU/ml at 48 hpi (Fig. 2C, D, and E), indicating that transfection of small RNAs does not interfere with viral replication. Following transfection with miR-1271-5p and miR-1307-3p mimics and inhibitors, WNV_{KUN} titers at all time points were similar to those of the control, indicating that the miRNAs did not influence viral replication (Fig. 2D and E). In contrast, the WNV_{KUN} titer was significantly reduced in cells transfected with the miR-532-5p mimic and increased in cells transfected with the miR-532-5p inhibitor (Fig. 2C). Virus replication in cells transfected with the miR-532-5p mimic was inhibited by approximately 10-fold at 48 hpi and enhanced by ~8-fold in cells transfected with the corresponding miRNA inhibitor at 24 hpi (Fig. 2C). The differences in both cases diminished by 72 hpi (96 hpt) (Fig. 2C), likely due to the observed decline in the intracellular levels of the mimic and inhibitor (Fig. 2A and B). The observed changes in WNV_{KUN} replication efficiency in cells transfected with miR-532-5p mimic or inhibitor provide strong evidence for the antiviral activity of miR-532-5p.

The antiviral effect of miR-532-5p is not mediated by interactions between the miRNA and putative complementary sites in WNV_{KUN} genomic RNA. Host miRNAs were shown to influence the life cycles of RNA viruses either by altering the host gene expression (50, 51) or by binding directly to viral RNA (13, 16, 52). To determine whether miR-532-5p inhibits WNV_{KUN} replication via direct interaction with viral RNA, computational screening of viral RNA for the potential miR-532-5p binding sites was performed. Analysis conducted using RNA Hybrid software identified two potential miR-532 binding sites in WNV_{KUN} genomic RNA (Fig. 3A). These predictions were then experimentally validated using a luciferase reporter assay. Nucleotide sequences from WNV_{KUN} RNA predicted to interact with miR-532-5p were inserted into the 3′ UTR of *f-luc* in the pmirGLO target vector. Constructs containing insertions with 100% complementarity to miR-532-5p and a scrambled miR-532-5p target sequence were also generated and used as a positive and a negative control, respectively.

HEK293 cells were cotransfected with reporter constructs and miR-532-5p mimics, followed by a luciferase activity assay at 24 hpt. In cells transfected with the positive-control reporter construct, luciferase expression was reduced by ~60% in the presence of the miR-532-5p mimic compared to cells transfected with a nonspecific mimic. Transfection of the miRNA mimic had no effect on expression of luciferase from the scrambled reporter construct (Fig. 3B). These results demonstrate that the miR-532-5p mimic was efficiently incorporated into RISC and guided it to the complementary region of the target mRNA in a sequence-specific manner. However, transfection of miR-532-5p mimics did not alter the expression of luciferase from reporter constructs

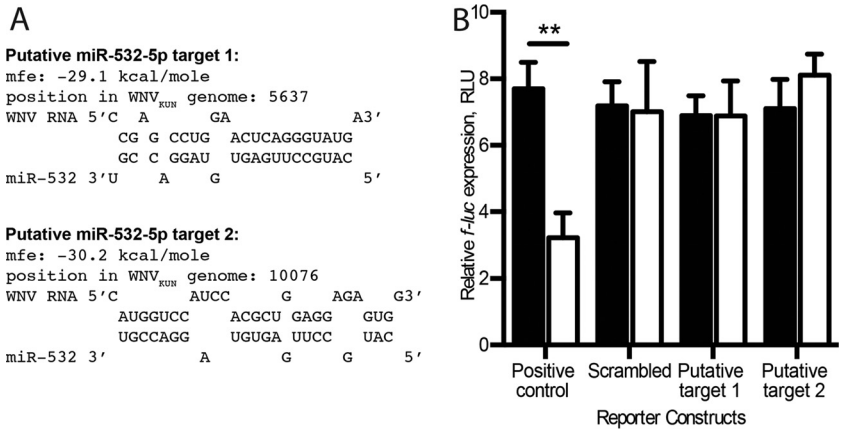

FIG 3 WNV$_{KUN}$ genomic RNA is not the target of miR-532-5p. (A) Predicted interactions between miR-532-5p and WNV$_{KUN}$ genomic RNA. (B) Effect of miR-532-5p mimic on expression of the firefly luciferase gene (*f-luc*) from miRNA sensor constructs. Sequences of predicted target sites in the WNV$_{KUN}$ genome (putative target 1 or 2) were inserted into the 3′ UTR of the *f-luc* gene in the pmirGLO dual-luciferase reporter vector. Sequences with full complementarity to miR-532-5p sequence or with scrambled (random nucleotides) sequence were inserted into the same region to create positive and negative (scrambled) control vectors. HEK293 cells were cotransfected with reporter constructs and the miR-532-5p or nonspecific miRNA mimics. The values are expressed as relative *f-luc* expression calculated as a ratio of *f-luc* to *r-luc* (*Renilla* luciferase) activity (RLU, relative light units). The values are the means of three independent experiments, with the error bars showing standard deviations. **, $P < 0.01$.

bearing either of the predicted miR-532-5p target sites from the WNV$_{KUN}$ RNA (Fig. 3B). Therefore, the mechanism by which miR-532-5p inhibits virus replication is likely to involve miR-532-5p-mediated regulation of host genes.

MicroRNA miR-532-5p inhibits expression of SESTD1 and TAB3 in WNV$_{KUN}$-infected cells. To elucidate which host genes are targeted by miR-532-5p, genome-wide computational prediction of all potential miR-532-5p targets was performed. To minimize the number of false-positive predictions, the analysis was performed using 6 different prediction algorithms, and only interactions predicted by at least 5 of them were considered for further analysis. The algorithms used were based on evolutionary conservation of sites (miRDB and TargetScanHuman), seed complementarity (DIANA-MicroT and microRNA.org), and the thermodynamics of duplexes (TargetMiner and RNA22). Each of the algorithms predicted a substantial number of putative miR-532-5p targets, ranging from 215 to 19,195 targets; however, only 10 of these (CPEB3, FAM116A, SESTD1, RASSF5, GBP1, ZNF536, RAB11A, ARMC8, SMAD2, and TAB3) were simultaneously predicted by at least 5 different algorithms (Table 5). These putative targets of miR-532-5p, together with previously characterized target genes listed in the MirTarBase database (TRAPPC2P1, METTL20, ZFHX3, and CPNE1), were selected for experimental analysis of their contributions to the miR-532-5p-mediated antiviral effect.

Taking into account that miRNAs typically inhibit the expression of target genes, the inverse correlation between the expression of an miRNA and interacting mRNAs can be used for exper-

TABLE 5 miR-532-5p putative target sites in the 3′ UTRs of human mRNA transcripts predicted using different algorithms

Gene	GenBank accession no.	Target site(s) for prediction algorithm[a]: miRDB	TargetScan	DIANA	microRNA.org	TargetMiner	RNA22
CPEB3	NM_001178137	1025, 2156, 3005	1025, 2156, 3005	1003–1031, 2134–2162, 2983– 3011	1011, 2124, 2991		
FAM116A	NM_152678		2706, 223, 707, 1193	201–229, 887–915, 2684–2712, 685–713, 1171–1199	208, 693, 895, 1179, 2695	915, 2196, 2712, 1946, 713, 553, 229, 2229	223, 707, 1193
SESTD1	NM_178123	161, 919, 7813	161, 919, 4838, 7813, 7850	159–167, 917–925		926, 168	161, 919, 7813
RASSF5	NM_182663	684, 1891, 2002	684, 19891, 2002	1999–2027, 792–820, 2110–2138	669, 1873, 1987	1721, 1897, 2009, 691	684, 19891, 2002
GBP1	NM_002053	30,121	30, 121	28–36, 119–127, 1757–1765	18, 107		30, 121
ZNF536	NM_014717	717	717	715–723			717
RAB11A	NM_001206836	1072, 1421	1160, 1509	1050–1078, 910–938, 1399–1427			1050
ARMC8	NM_014154		59	57–65, 124–132		66, 1386	59
SMAD2	NM_001003652	4083, 6655	6655, 4083	4500–4528, 4061–4089, 6633–6661	-	7826, 7782, 2090, 1625, 258, 7186, 1058, 662	4083, 6655, 662
TAB3	NM_152787	3271, 3886	3271, 3886, 627		612, 3257, 3873	3646, 2948, 633, 3892, 3278	3271, 3886, 627
DHX9	NM_001357		30	22–50	30		30

[a] The numbers represent nucleotide positions in the 3′ UTRs of the respective mRNAs. For all algorithms but DIANA, the numbers indicate the first nucleotide of binding sites. The numbers for the DIANA algorithm represent the first and last nucleotides of binding sites.

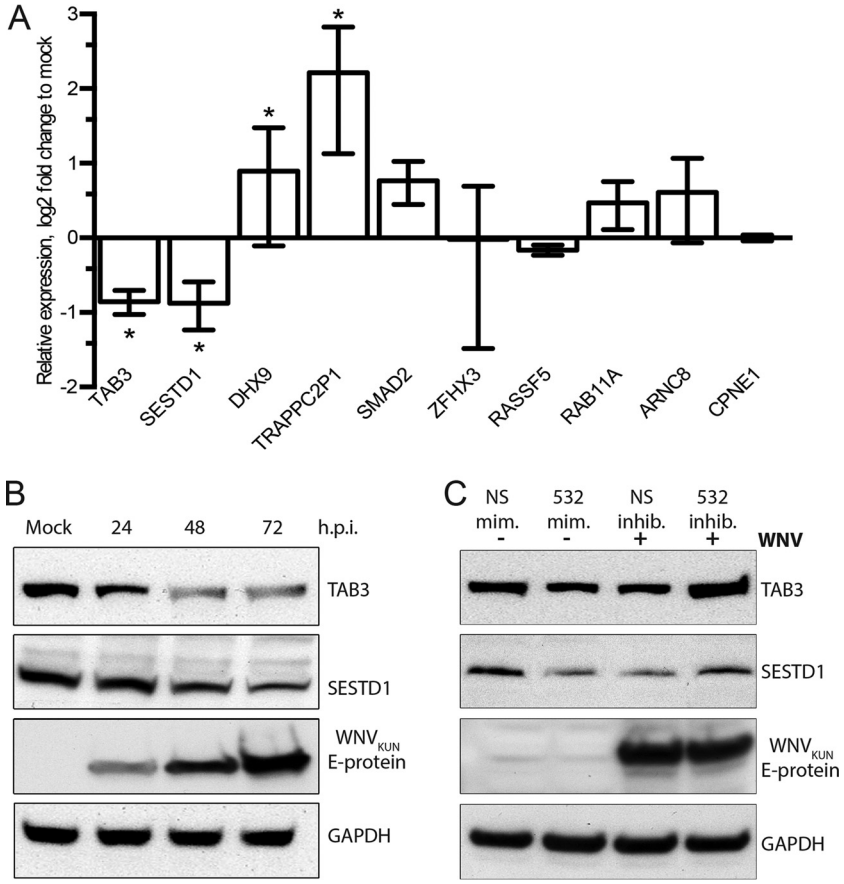

FIG 4 Experimental validation of predicted miR-532-5p targets. (A) Expression of predicted miR-532-5p targets in WNV_{KUN}-infected HEK293 cells determined by qRT-PCR. Relative expression is represented as log_2-fold change compared to an uninfected control. The means of three biological replicates with technical triplicates are shown. The error bars show standard deviations. *, $P < 0.05$. (B) Western blot detection of TAB3 and SESTD1 in HEK293 cells at 24 h, 48 h, and 72 h after infection with WNV_{KUN} at an MOI of 1. The GAPDH blot was used as a loading control, and WNV_{KUN} E protein antibodies were used to detect virus infection. (C) Effects of miR-532-5p mimic and inhibitor on expression of TAB3 and SESTD1 in mock- and WNV_{KUN}-infected cells. HEK293 cells were transfected with miR-532-5p mimic (532 mim.), miR-532-5p inhibitor (532 inhib.), or nonspecific control RNA mimic (NS mim.) or inhibitor (NS inhib.). At 24 h posttransfection, the cells transfected with mimics were lysed and the cells transfected with inhibitors were infected with WNV_{KUN} at an MOI of 1 and then lysed at 36 h postinfection. Expression of TAB3, SESTD1, GAPDH (loading control), and WNV_{KUN} E protein (control for infection) was determined by Western blotting with the corresponding antibodies.

imental validation of predicted targets. To this end, we first determined the expression of predicted and previously validated miR-532-5p target genes in WNV_{KUN}-infected and uninfected HEK293 cells using qRT-PCR. The analysis demonstrated that WNV_{KUN} infection resulted in a significant decrease in mRNA levels for only two of the examined mRNAs, TAB3 and SESTD1 (Fig. 4A), suggesting that these mRNAs are likely to be targeted for degradation by upregulated miR-532-5p. In contrast, expression of the well-known antiviral genes (53) SMAD2 and GBP1 was increased by ~2-fold (Fig. 4A) and by ~90-fold (data not shown), respectively. Expression of the noncoding pseudoretrogene TRAPPC2P1 was also increased by ~4-fold (Fig. 4A). Therefore, even if miR-532 targets these transcripts, the effect of miRNA-532 on their expression is negligible compared to those of other regulatory mechanisms that drive their upregulation during infection. Thus, they are unlikely to be the miR-532 targets that mediate the antiviral effect of this miRNA. The levels of CPNE1, RASSF5, RAB11A, DHX9, ARMC8, and ZFHX3 mRNAs were not significantly altered by infection (Fig. 4A), while FAM116A, METTL20P, CPEB3, and ZNF536 mRNAs were below the limit of detection in both infected and uninfected cells.

As miRNA-mediated gene repression occurs predominantly at the translational level and has a more prominent effect on the level of protein, we also determined the effect of WNV_{KUN} infection on TAB3 and SESTD1 protein levels. HEK293 cells were infected with WNV_{KUN} at an MOI of 1, and the TAB3 and SESTD1 proteins were detected by Western blotting with specific antibodies at 24, 48, and 72 hpi. TAB3 protein levels were reduced in infected cells compared to an uninfected control at all analyzed time points, and SESTD1 protein levels were decreased at later time points (48 and 72 hpi) (Fig. 4B). These results provided additional evidence for downregulation of putative miR-532-5p target genes, TAB3 and SESTD1, in infected cells.

To determine if downregulation of TAB3 and SESTD1 in infected cells was indeed mediated by miR-532-5p, we assessed the effect of miR-532-5p mimic transfection on TAB3 and SESTD1 protein levels and also examined the ability of miR-532-5p inhibitor to restore diminished expression of these genes in infected

cells. HEK293 cells were transfected with miR-532-5p-specific or nonspecific miRNA mimics, and at 24 hpt, expression of TAB3 and SESTD1 was analyzed by Western blotting, followed by quantification of detected protein bands using digital densitometry. Transfection of miR-532 mimic resulted in approximately 60% and 40% reduction in SESTD1 and TAB3 expression, as determined by densitometry of two independent blots (Fig. 4C), which was comparable to the corresponding reductions in the levels of these proteins observed in infected cells at 24 hpi (Fig. 4B). The results demonstrated that miR-532-5p also downregulated SESTD1 and TAB3 expression in the absence of WNV_{KUN} infection.

In order to confirm that the inhibitory effect of miR-532-5p on TAB3 and SESTD1 expression is indeed responsible for their downregulation in response to WNV_{KUN} infection, HEK293 cells were transfected with miR-532-5p inhibitor or a nonspecific inhibitor and subsequently infected with WNV_{KUN} at 24 hpt. At 36 hpi (60 hpt), TAB3 and SESTD1 levels were determined by Western blotting. Transfection with miR-532-5p inhibitor resulted in restoration of both proteins to the levels observed in uninfected cells (Fig. 4C, compare lanes NS mim. and 532 inhib.). The results show that downregulation of TAB3 and SESTD1 expression by WNV_{KUN} infection can be reversed by inhibiting miR-532-5p function using a miR-532-5p-specific inhibitor. Taken together, these results demonstrate that upregulation of miR-532-5p expression in WNV-infected cells leads to mir-532-5p-specific inhibition of TAB3 and SESTD1 expression.

Mir-532-5p targets the 3′ UTRs of SESTD1 and TAB3 transcripts. The suppressive effect of miR-532-5p on the expression of TAB3 and SESTD1 is likely to result from direct miRNA interaction with the binding sites located in the 3′ UTRs of the corresponding mRNAs with subsequent translational repression and/or mRNA degradation. Alternatively, the effect could be indirect, mediated by miR-532-5p interaction with other potential targets that in turn could influence the expression of TAB3 and SESTD1. Our *in silico* analysis suggested three putative binding sites for miR-532-5p in the 3′ UTRs of each of the TAB3 and SESTD1 mRNAs (Fig. 5A). To determine if miR-532-5p can directly interact with these sites and inhibit the expression of targeted genes, a luciferase reporter assay was used. All three putative miR-532-5p target sites from the TAB3 or SESTD1 3′ UTR separated by 20-nucleotide spacers were inserted into the 3′ UTR of the *f-luc* gene in the pmirGLO target vector. The scrambled target sequences were used to create corresponding negative-control reporter plasmids. HEK293 cells were cotransfected with reporter constructs and either miR-532-5p mimic or nonspecific miRNA mimic, and at 24 hpt, luciferase activity was measured. Transfection of the miR-532-5p mimic significantly reduced the expression of the luciferase gene carried by the pmiRGLO-TAB3-Target or pmiR-GLO-SESTD1-Target reporter construct, but not that carried by the corresponding scrambled controls (Fig. 5B). Approximately 2- to 3-fold reduction in *f-luc* activity was observed in cells transfected with pmiR-GLO plasmids bearing the putative miR-532-5p target sites from each gene (Fig. 5B), which was comparable with the effect observed using a reporter construct encoding a target site with 100% complementarity to the miR-532-5p sequence (Fig. 3B). The results of reporter assays showed direct interaction of miR-532-5p with predicted target sites in the 3′ UTRs of TAB3 and SESTD1 mRNAs. Collectively, the results of the reporter assays discussed here and of the miR-532-5p mimic and inhibitor assays discussed above demonstrate that SESTD1 and TAB3 represent novel targets of miR-532-5p that are downregulated by the miRNA in response to WNV_{KUN} infection.

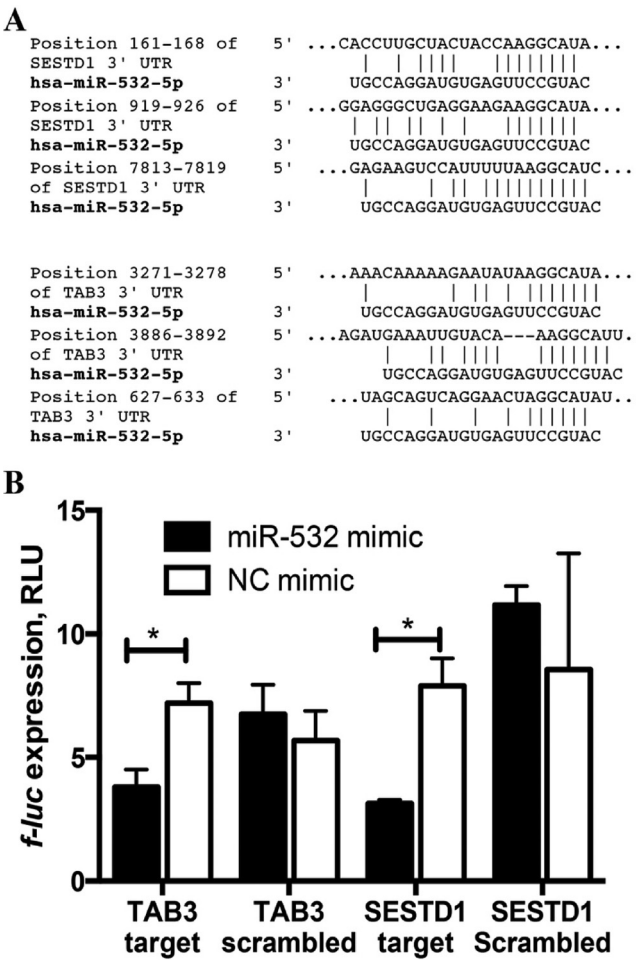

FIG 5 MiR-532-5p interacts with predicted target sites in the 3′ UTRs of TAB3 and SESTD1 mRNAs. (A) Predicted target sites for miR-532-5p in the 3′ UTRs of TAB3 and SESTD1. Nucleotide positions in the corresponding 3′ UTRs that are complementary to the miR-532-5p seed region are indicated. Vertical lines show complementary interactions. (B) Effect of miR-532-5p mimic on expression of the firefly luciferase gene (*f-luc*) from reporter constructs containing in the *f-luc* 3′ UTR the putative miR-532-5p binding sites from the TAB3 and SESTD1 3′ UTRs. Constructs with scrambled TAB3 and SESTD1 sequences inserted in the 3′ UTR of *f-luc* were used as negative controls. The values are the means of the results of three independent experiments, with the error bars showing standard deviations. *, $P < 0.05$.

SESTD1 and TAB3 are required for WNV_{KUN} replication. In order to elucidate the role of SESTD1 and TAB3 in WNV_{KUN} infection, we assessed viral replication in cells depleted of SESTD1 and TAB3 by siRNAs. HEK293 cells were transfected with three siRNAs specific to SESTD1 or TAB3 or with nonspecific siRNAs. The efficiency of siRNA-mediated SESTD1 and TAB3 knockdown was first determined by Western blotting at 24, 48, 72, and 96 hpt. SESTD1 knockdown was very efficient, with 80% decrease in SESTD1 expression at 24 hpt and further decrease to an undetectable level at 48 and 72 hpt (Fig. 6A). TAB3 knockdown was somewhat less efficient, with no apparent reduction at 24 hpt and ~50 to 60% reduction at 48 and 72 hpt (Fig. 6B). Expression of both

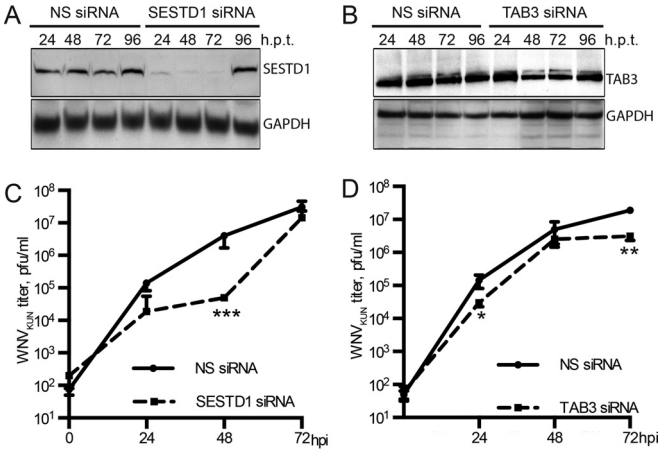

FIG 6 Effect of SESTD1 or TAB3 depletion on WNV_{KUN} replication. (A and B) Knockdown of SESTD1 (A) and TAB3 (B) in HEK293 cells by siRNAs. Nonspecific (NS) siRNAs were used as negative controls. (C and D) Effects of SESTD1 (C) and TAB3 (D) knockdown on WNV_{KUN} replication. At 24 h after transfection with SESTD1 (B) or TAB3 (D) siRNA or NS siRNA, cells were infected with WNV_{KUN} at an MOI of 0.1, and virus titers in the culture fluid collected at the indicated times after infection were determined by plaque assay on BHK-21 cells. The values in panels C and D are means of three biological replicates with technical duplicates. The error bars show standard deviations. *, $P < 0.05$; **, $P < 0.01$; ***, $P < 0.001$.

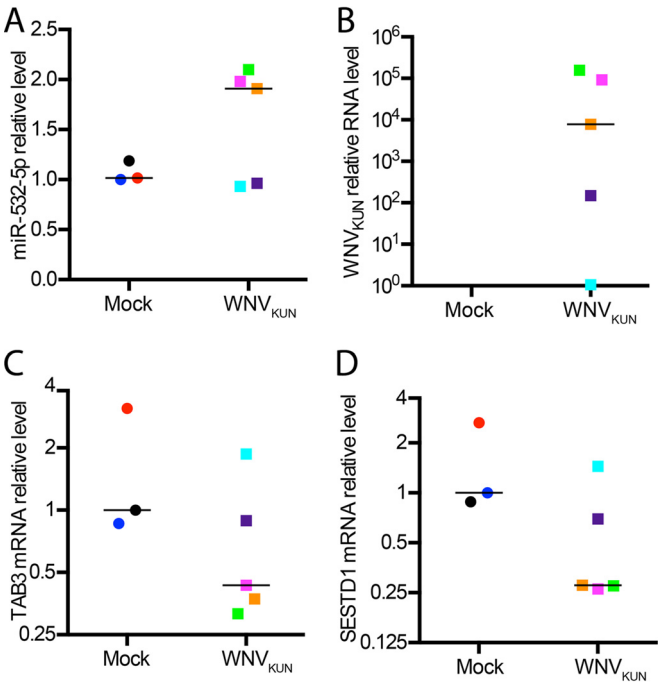

FIG 7 Effects of WNV_{KUN} infection on expression of miR-532, TAB3, and SESTD1 in mouse brains. Relative levels of RNAs in the total brain RNA of infected mice were determined by the $\Delta\Delta C_T$ method with comparison to the levels in the brains of uninfected animals. Normalized levels of RNAs in samples from individual animals and median levels in the groups are shown. (A) Levels of miR-532 were determined by SL-qRT-PCR and normalized to the miR-30e-3p level. (B to D) Levels of WNV genomic RNA (B), TAB3 mRNA (C), and SESTD1 mRNA (D) were determined by qRT-PCR with normalization to the TBP mRNA levels. All experiments included duplicates for RT reactions and technical triplicates for qPCR.

SESTD1 and TAB3 recovered by 96 hpt (Fig. 6A and B). To determine the effect of depletion on virus infection, cells transfected with siRNAs were infected at an MOI of 0.1 with WNV_{KUN} at 24 hpt. Samples of culture fluid from the infected cells were collected at 24, 48, and 72 hpi (or at 48, 72, and 96 hpt, respectively), and WNV_{KUN} titers were determined by plaque assay on BHK-21 cells. The most significant effect of SESTD1 depletion on virus infection was observed at 48 hpi (72 hpt), when WNV_{KUN} titers were reduced by ~100-fold (Fig. 6C). The effect was largely gone by 72 hpi (96 hpt), when SESTD1 expression had already recovered (Fig. 6C). Following TAB3 depletion, statistically significant reduction in WNV_{KUN} titers was observed at 24 hpi (48 hpt), while the most significant reduction (~10-fold) was observed at 72 hpi (96 hpt), when TAB3 expression largely recovered (Fig. 6D). The results show the roles of both SESTD1 and TAB3 in controlling WNV_{KUN} infection, with SESTD1 likely to play a more significant and direct role, while the antiviral function of TAB3 appears to be less prominent and/or may require another host factor influenced by TAB3.

Upregulation of miR-532 and downregulation of TAB3 and SESTD1 in response to WNV_{KUN} infection also occur *in vivo*. In order to determine whether miR-532 upregulation by WNV infection and its inhibitory effect on TAB3 and SESTD1 expression also occur in other cells/tissues, we performed corresponding analyses in brains of WNV-infected mice. Mouse miR-532 has 100% homology to the human miRNA. In addition, two out of three miR-532 binding sites in TAB3 and SESTD1 mRNAs were found to be evolutionarily conserved in vertebrates by computational analysis used for target prediction. A group of 21-day-old mice ($n = 5$) were infected with 10^4 PFU of WNV_{KUN} (strain NSW2011), with a group of uninfected mice ($n = 3$) used as controls. The infected animals showing symptoms of encephalitis were euthanized, and RNA was isolated from their brains. Uninfected mice, where possible, were sacrificed on the same day as encephalitic animals. Expression of miR-532, TAB3, and SESTD1 mRNAs and viral RNA in the brains was assessed by qRT-PCR (Fig. 7). Elevated levels (by ~2-fold) of miR-532 were detected in the brains of 3 out of the 5 infected mice (Fig. 7A). These animals were also the first to develop symptoms of encephalitis and had the highest levels of viral RNA in the brain, whereas the animals that did not show increased miR-532 expression had no or a low level of WNV RNA (Fig. 7B). This indicates that upregulation of miR-532 in response to WNV is not limited to HEK293 cells and also occurs *in vivo* in infected mice. We also assessed the expression of miR-532 targets, TAB3 and SESTD1, in the brains of infected and uninfected animals. The decreased expression of TAB3 (by ~3-fold) and SESTD1 (by ~4-fold) was observed in the brains with elevated levels of miR-532 and high levels of WNV RNA. This further confirms the effect of WNV infection on TAB3 and SESTD1 expression and suggests a role of miR-532 in downregulation of these genes *in vivo*.

DISCUSSION

In addition to their critical role in regulating normal cellular gene expression, the significance of miRNAs in virus-host interactions is becoming evident. The activity of host miRNAs can drastically influence the virus life cycle, either by facilitating enhanced replication (20) or by mediating the host antiviral response (24). Therefore, it is not surprising that viruses, including WNV, modulate the expression of specific cellular miRNAs (6, 7, 32). WNV is a significant human pathogen causing disease outbreaks with fatal

outcomes (3). Despite this, the roles of host miRNAs in WNV-host interactions and pathogenesis have not been extensively studied. Previously, we demonstrated that the mosquito miRNA aae-miR-2940 is downregulated in response to WNV_{KUN} infection, which results in inhibition of virus replication in insect cells. In the current study, the role of miRNAs in response to WNV_{KUN} infection in mammalian cells was addressed.

In order to identify miRNAs that may be involved in WNV-host interactions, we first compared the miRNA expression profiles in uninfected and WNV_{KUN}-infected HEK293 cells at 24 and 48 hpi. The effect of WNV infection on expression of miRNAs in HEK293 cells was previously evaluated using microarray (6) and medium-throughput qRT-PCR (7) analyses. This resulted in identification of somewhat different patterns of differentially expressed miRNAs in the two studies, which could be due to biases and limitations of the methods implemented. In our study, we employed RNA-seq analysis, which not only provides data on the relative expression of each miRNA compared to the control sample, but also allows the absolute quantification of miRNAs in each sample. We found that the majority of miRNAs that exhibited differential expression in infected cells were represented by only tens or hundreds of reads per million, which is less than 0.1% of the total miRNA pool, the amount considered a cutoff for miRNA levels that can exhibit any meaningful biological activity (49). Only 24 cellular miRNAs that were expressed at levels equal to or higher than 1,000 reads per million were shown to be differentially expressed in WNV_{KUN}-infected cells, with changes in expression ranging from 0.5 to 2 $\log_2$-fold (1.5- to 4-fold). To gain better insight into the molecular mechanisms involved in differential expression of human miRNAs in response to WNV_{KUN} infection, we also determined the expression of pre-miRNAs. Interestingly, the expression of the overwhelming majority of these 24 pre-miRNAs was upregulated in infected cells, while the expression of 17 of the 24 mature miRNAs processed from these pre-miRNAs was downregulated. This indicates that a combination of transcriptional and posttranscriptional mechanisms determine the miRNA response to WNV_{KUN} infection. We focused our attention on seven miRNAs (miR-1271-5p, miR-151b, miR-24-3p, miR-25-3p, miR-33-3p, miR-1307-5p, and miR-532-5p) that had increased levels of both mature miRNAs and pre-miRNAs. The rationale for choosing these miRNAs was based on our intent to focus only on those miRNAs that were upregulated at the initial transcriptional level as a consequence of direct host response to infection rather than on those miRNAs for which the pre-miRNA-to-miRNA processing could be affected by a rather nonspecific mechanism that might involve previously shown WNV-mediated inhibition of Dicer activity (54, 55). The expression of these seven miRNAs was then validated using qRT-PCR and Northern blot analyses, which demonstrated a significant increase in expression for only 3 of the miRNAs—miR-1271-5p, miR-1307-5p, and miR-532-5p.

In order to determine the biological roles of these upregulated miRNAs in the host response to infection, the effects of miR-1271-5p, miR-1307-5p, and miR-532-5p on WNV_{KUN} replication were assessed using corresponding miRNA mimics. Only miR-532-5p exhibited a significant antiviral effect, while miR-1271-5p and miR-1307-5p did not affect viral replication. The fact that miR-532-5p is an antiviral miRNA induced in response to WNV_{KUN} infection is the key new finding of our study. The differential expression of this miRNA was previously observed in response to infection with chikungunya virus (CHIKV) (51) and simian immunodeficiency virus (SIV) (56). However, the direct antiviral role of miR-532-5p against these and other viruses has not yet been demonstrated.

Host miRNAs were previously shown to interact directly with viral RNAs of RNA viruses such as hepatitis C virus (17, 57), eastern equine encephalitis virus (13), and enterovirus 71 (16) and to modulate virus replication. However, whether biologically relevant direct interactions between host miRNAs and viral genomic RNAs occur widely in nature is currently the subject of debate (58, 59). Our data obtained using reporter assays showed that mir-532-5p does not directly interact with the 2 predicted sites in WNV_{KUN} RNA, suggesting that the antiviral effect exhibited by the miRNA is mediated by its interactions with the host mRNA transcripts. Indeed, our data showed that two of the predicted host targets of miR-532-5p, SESTD1 and TAB3, interacted with miR-532-5p and that their expression was downregulated by these interactions in reporter assays, as well as in WNV_{KUN}-infected cells. This is the first experimental identification and validation of SESTD1 and TAB3 as miR-532-5p targets. The stringent criteria used in target prediction and validation ensured the reliability of identified targets. However, we cannot exclude the possibility that some potential miR-532 targets with lower miRNA binding affinity/evolutionary conservation could have been overlooked due to the high data filtration stringency. Interestingly, the previously characterized mir-532 target genes listed in the MirTarBase database (TRAPPC2P1, METTL20, ZFHX3, and CPNE1) were not predicted by 5 out of the 6 algorithms (the stringent selection criteria used in our study), and their expression was also shown not to be reduced in WNV_{KUN}-infected cells (Fig. 4A).

In order to elucidate how the products of these genes influence viral replication and if their suppression by miR-532-5p is responsible for the antiviral activity of the miRNA, we employed siRNA knockdown to assess WNV_{KUN} replication in SESTD1- and TAB3-depleted cells. The knockdown experiment demonstrated that both proteins are required for WNV_{KUN} replication in human cells, with SESTD1 depletion having a more profound inhibitory effect on virus replication than TAB3 depletion. We also demonstrated that upregulation of miR-532 expression and downregulation of TAB3 and SESTD1 occur in the brains of mice in response to WNV_{KUN} infection.

SESTD1 is a phospholipid-binding protein containing a lipid-binding SEC14-like domain and two spectrin repeat cytoskeleton interaction domains, localized in the plasma membrane, which binds several phospholipid species and is essential for efficient activation of the channels TRPC4 and TRPC5 (60). Calcium transport was previously shown to be required for efficient propagation of WNV (61). WNV infection was shown to lead to rapid and sustained Ca^{2+} influx through Ca^{2+} channels and endocytosis (61). Calcium transport depletion by specific inhibitors of Ca^{2+} channels and the Ca^{2+}-binding protein CB-D28k were shown to have a strong inhibitory effect on WNV replication (61, 62). Ca^{2+} influx is thought to be required for early stages of virus replication (possibly for virus-induced rearrangement of the endoplasmic reticulum membrane) and for later infection stages, when Ca^{2+}-dependent activation of caspase 3 cleavage leads to decreased activation of the FAK and ERK1/2 pathways, extending the survival of WNV-infected cells (62). Taking into account the demonstrated role of SESTD1 in activation of Ca^{2+} channels and the previously demonstrated importance of Ca^{2+} influx in WNV

replication, it is likely that the main molecular mechanism of miR-532-5p-mediated antiviral activity involves inhibition of Ca^{2+} influx through suppression of SESTD1 expression. We propose that as a part of the host response to infection, downregulation of SESTD1 by mir-532 may lower the influx of Ca^{2+} but not completely block it. It is likely that SESTD1-independent Ca^{2+} channels that also operate in cells can contribute to the overall Ca^{2+} influx observed in flavivirus-infected cells. Inhibition of SESTD1 by mir-532, however, may decrease Ca^{2+} accumulation to a level sufficient to inhibit or delay Ca^{2+}-dependent processes required for virus replication. However, validation of this hypothesis requires further extensive experimentation.

TAB3/MAP3K7IP3 (transforming growth factor beta [TGF-β]-activated kinase binding protein 3/mitogen-activated protein kinase kinase kinase 7 interacting protein 3) is an adaptor protein that forms a tertiary complex with the protein kinase MAP3K7/TAK1 and TRAF2 or TRAF6 in the interleukin 1 (IL-1) and TNF signaling pathways (63). It acts cooperatively with another adaptor protein from the TAB family, TAB1, and is functionally redundant to TAB2. TAB3 mediates activation of TAK1 kinase, which in turn phosphorylates c-Jun N-terminal kinases (JNKs) and the IkBα/β subunit of NF-κB. This leads to activation of the transcription factors AP-1 and NF-κB and their nuclear translocation (64). TAK-1 signaling contributes to a variety of cellular and tissue pathophysiologies, including cell survival, proliferation, differentiation, embryonic development, inflammation, and carcinogenesis (65). Activation of the TAB/TAK/NF-κB pathway has been shown to inhibit apoptosis and promote cell survival (66, 67). Human immunodeficiency virus type 1 (HIV-1) activates TAK-1 in order to promote replication via NF-κB- and AP-1-dependent induction of the cytokines IL-6, IL-8, and CCL5, as well as increased transcription of viral genes (68). TAB3 was shown to be essential for activation of TAK-1 by HIV-1 (68). Considering the important role of TAB3 in regulation of cell survival and induction of anti-inflammatory cytokines, it is possible that miR-532-5p-mediated suppression of TAB3 expression may promote apoptosis of WNV-infected cells, contributing to the antiviral effect of miR-532-5p. Interestingly, in contrast to the observed profound and immediate effect of SESTD1 depletion on WNV_{KUN} replication, the antiviral effect of TAB3 depletion was less profound and also appeared to be delayed. Notably, however, TAB3 depletion by siRNAs was less efficient than SESTD1 depletion, which may explain, at least in part, the less efficient antiviral effect. It is also possible that redundancy in the TAB family of proteins could contribute to the less profound antiviral effect of TAB3 depletion, while the delay in the antiviral effect of TAB3 depletion may be caused by its indirect effect on activation of downstream host factors in this signaling pathway.

In summary, this study demonstrates that miR-532-5p is upregulated in response to WNV_{KUN} infection in human cells and mouse brain tissue. Subsequently, upregulated miR-532-5p suppresses the expression of SESTD1 and TAB3 genes via targeting of their 3′ UTR sequences. These genes are required for efficient WNV_{KUN} replication, likely due to their roles in Ca^{2+} influx and regulation of cell survival. The overall effect of the miR-532-5p-mediated host response is the suppression of virus replication. These findings further highlight the important role of mammalian miRNAs in antiviral response and may have important implications for understanding the molecular mechanisms that determine flavivirus-host interactions and pathogenesis.

ACKNOWLEDGMENTS

We acknowledge Roy Hall (University of Queensland) for providing antibody to the WNV_{KUN} E protein, Brian Clarke (University of Queensland) for critical reading of the manuscript, and all other members of A.A.K.'s laboratory for useful discussions.

This work was supported by NHMRC grant 1027110. A.A.K. is a Senior Research Fellow with the NHMRC.

FUNDING INFORMATION

This work was funded by Department of Health | National Health and Medical Research Council (NHMRC) under grant 1027110.

REFERENCES

1. **Chancey C, Grinev A, Volkova E, Rios M.** 2015. The global ecology and epidemiology of West Nile virus. Biomed Res Int **2015:**376230. http://dx.doi.org/10.1155/2015/376230.
2. **Kilpatrick AM.** 2011. Globalization, land use, and the invasion of West Nile virus. Science **334:**323–327. http://dx.doi.org/10.1126/science.1201010.
3. **Hall RA, Broom AK, Smith DW, Mackenzie JS.** 2002. The ecology and epidemiology of Kunjin virus. Curr Top Microbiol Immunol **267:**253–269.
4. **Frost MJ, Zhang J, Edmonds JH, Prow NA, Gu X, Davis R, Hornitzky C, Arzey KE, Finlaison D, Hick P, Read A, Hobson-Peters J, May FJ, Doggett SL, Haniotis J, Russell RC, Hall RA, Khromykh AA, Kirkland PD.** 2012. Characterization of virulent West Nile virus Kunjin strain, Australia, 2011. Emerg Infect Dis **18:**792–800. http://dx.doi.org/10.3201/eid1805.111720.
5. **Suthar MS, Diamond MS, Gale M.** 2013. West Nile virus infection and immunity. Nat Rev Microbiol **11:**115–128. http://dx.doi.org/10.1038/nrmicro2950.
6. **Smith JL, Grey FE, Uhrlaub JL, Nikolich-Zugich J, Hirsch AJ.** 2012. Induction of the cellular microRNA, Hs_154, by West Nile virus contributes to virus-mediated apoptosis through repression of antiapoptotic factors. J Virol **86:**5278–5287. http://dx.doi.org/10.1128/JVI.06883-11.
7. **Chugh PE, Damania BA, Dittmer DP.** 2014. Toll-like receptor-3 is dispensable for the innate microRNA response to West Nile virus (WNV). PLoS One **9:**e104770. http://dx.doi.org/10.1371/journal.pone.0104770.
8. **Carthew RW, Sontheimer EJ.** 2009. Origins and mechanisms of miRNAs and siRNAs. Cell **136:**642–655. http://dx.doi.org/10.1016/j.cell.2009.01.035.
9. **Bartel DP.** 2009. MicroRNAs: target recognition and regulatory functions. Cell **136:**215–233. http://dx.doi.org/10.1016/j.cell.2009.01.002.
10. **Cheng Y, Kuang W, Hao Y, Zhang D, Lei M, Du L, Jiao H, Zhang X, Wang F.** 2012. Downregulation of miR-27a* and miR-532-5p and upregulation of mir-146a and mir-155 in LPS-induced RAW264.7 macrophage cells. Inflammation **35:**1308–1313. http://dx.doi.org/10.1007/s10753-012-9443-8.
11. **Jia X, Bi Y, Li J, Xie Q, Yang H, Liu W.** 2015. Cellular microRNA miR-26a suppresses replication of porcine reproductive and respiratory syndrome virus by activating innate antiviral immunity. Sci Rep **5:**10651. http://dx.doi.org/10.1038/srep10651.
12. **Zhao F, Xu G, Zhou Y, Wang L, Xie J, Ren S, Liu S, Zhu Y.** 2014. MicroRNA-26b inhibits hepatitis B virus transcription and replication by targeting the host factor CHORDC1 protein. J Biol Chem **289:**35029–35041. http://dx.doi.org/10.1074/jbc.M114.589978.
13. **Trobaugh DW, Gardner CL, Sun C, Haddow AD, Wang E, Chapnik E, Mildner A, Weaver SC, Ryman KD, Klimstra WB.** 2014. RNA viruses can hijack vertebrate microRNAs to suppress innate immunity. Nature **506:**245–248. http://dx.doi.org/10.1038/nature12869.
14. **Ahluwalia JK, Khan S, Soni K, Rawat P, Gupta A, Hariharan M, Scaria V, Lalwani M, Pillai B, Mitra D, Brahmachari SK.** 2008. Human cellular microRNA hsa-miR-29a interferes with viral nef protein expression and HIV-1 replication. Retrovirology **5:**117. http://dx.doi.org/10.1186/1742-4690-5-117.
15. **Gunasekharan V, Laimins LA.** 2013. Human papillomaviruses modulate microRNA 145 expression to directly control genome amplification. J Virol **87:**6037–6043. http://dx.doi.org/10.1128/JVI.00153-13.
16. **Zheng Z, Ke X, Wang M, He S, Li Q, Zheng C, Zhang Z, Liu Y, Wang H.** 2013. Human microRNA hsa-miR-296-5p suppresses enterovirus 71

replication by targeting the viral genome. J Virol **87:**5645–5656. http://dx.doi.org/10.1128/JVI.02655-12.
17. **Shimakami T, Yamane D, Jangra RK, Kempf BJ, Spaniel C, Barton DJ, Lemon SM.** 2012. Stabilization of hepatitis C virus RNA by an Ago2-miR-122 complex. Proc Natl Acad Sci U S A **109:**941–946. http://dx.doi.org/10.1073/pnas.1112263109.
18. **Campbell CL, Harrison T, Hess AM, Ebel GD.** 2014. MicroRNA levels are modulated in Aedes aegypti after exposure to Dengue-2. Insect Mol Biol **23:**132–139. http://dx.doi.org/10.1111/imb.12070.
19. **Qi Y, Li Y, Zhang L, Huang J.** 2013. MicroRNA expression profiling and bioinformatic analysis of dengue virus-infected peripheral blood mononuclear cells. Mol Med Rep **7:**791–798. http://dx.doi.org/10.3892/mmr.2013.1288.
20. **Wu S, He L, Li Y, Wang T, Feng L, Jiang L, Zhang P, Huang X.** 2013. miR-146a facilitates replication of dengue virus by dampening interferon induction by targeting TRAF6. J Infect **67:**329–341. http://dx.doi.org/10.1016/j.jinf.2013.05.003.
21. **Hayden MS, Ghosh S.** 2012. NF-κB, the first quarter-century: remarkable progress and outstanding questions. Genes Dev **26:**203–234. http://dx.doi.org/10.1101/gad.183434.111.
22. **Zhang G, Hussain M.** 2013. Wolbachia uses a host microRNA to regulate transcripts of a methyltransferase, contributing to dengue virus inhibition in Aedes aegypti. Proc Natl Acad Sci U S A **110:**10276–10281. http://dx.doi.org/10.1073/pnas.1303603110.
23. **Zhou Y, Liu Y, Yan H, Li Y, Zhang H, Xu J, Puthiyakunnon S, Chen X.** 2014. miR-281, an abundant midgut-specific miRNA of the vector mosquito Aedes albopictus enhances dengue virus replication. Parasit Vectors **7:**488. http://dx.doi.org/10.1186/s13071-014-0488-4.
24. **Zhu X, He Z, Hu Y, Wen W, Lin C, Yu J, Pan J, Li R, Deng H, Liao S, Yuan J, Wu J, Li J, Li M.** 2014. MicroRNA-30e* suppresses dengue virus replication by promoting NF-κB-dependent IFN production. PLoS Negl Trop Dis **8:**e3088. http://dx.doi.org/10.1371/journal.pntd.0003088.
25. **Wu N, Gao N, Fan D, Wei J, Zhang J, An J.** 2014. miR-223 inhibits dengue virus replication by negatively regulating the microtubule-destabilizing protein STMN1 in EAhy926 cells. Microbes Infect **16:**911–922. http://dx.doi.org/10.1016/j.micinf.2014.08.011.
26. **Wen W, He Z, Jing Q, Hu Y, Lin C, Zhou R, Wang X, Su Y, Yuan J, Chen Z, Yuan J, Wu J, Li J, Zhu X, Li M.** 2015. Cellular microRNA-miR-548g-3p modulates the replication of dengue virus. J Infect **70:**631–640. http://dx.doi.org/10.1016/j.jinf.2014.12.001.
27. **Escalera-Cueto M, Medina-Martínez I, del Angel RM, Berumen-Campos J, Gutiérrez-Escolano AL, Yocupicio-Monroy M.** 2015. Let-7c overexpression inhibits dengue virus replication in human hepatoma Huh-7 cells. Virus Res **196:**105–112. http://dx.doi.org/10.1016/j.virusres.2014.11.010.
28. **Zhu B, Ye J, Nie Y, Ashraf U, Zohaib A, Duan X, Fu ZF, Song Y, Chen H, Cao S.** 2015. MicroRNA-15b modulates Japanese encephalitis virus-mediated inflammation via targeting RNF125. J Immunol **195:**2251–2262. http://dx.doi.org/10.4049/jimmunol.1500370.
29. **Thounaojam MC, Kundu K, Kaushik DK, Swaroop S, Mahadevan A, Shankar SK, Basu A.** 2014. MicroRNA 155 regulates Japanese encephalitis virus-induced inflammatory response by targeting Src homology 2-containing inositol phosphatase 1. J Virol **88:**4798–4810. http://dx.doi.org/10.1128/JVI.02979-13.
30. **Sharma N, Verma R, Kumawat K, Basu A, Singh SK.** 2015. miR-146a suppresses cellular immune response during Japanese encephalitis virus JaOArS982 strain infection in human microglial cells. J Neuroinflammation **12:**30. http://dx.doi.org/10.1186/s12974-015-0249-0.
31. **Kumar M, Nerurkar VR.** 2014. Integrated analysis of microRNAs and their disease related targets in the brain of mice infected with West Nile virus. Virology **452-453:**143–151. http://dx.doi.org/10.1016/j.virol.2014.01.004.
32. **Slonchak A, Hussain M, Torres S, Asgari S, Khromykh AA.** 2014. Expression of mosquito microRNA aae-miR-2940-5p is downregulated in response to West Nile virus infection to restrict viral replication. J Virol **88:**8457–8467. http://dx.doi.org/10.1128/JVI.00317-14.
33. **Khromykh AA, Kenney MT, Edwin G, Westaway EG.** 1998. *trans*-Complementation of flavivirus RNA polymerase gene NS5 by using Kunjin virus replicon-expressing BHK cells. J Virol **72:**7270–7279.
34. **Chen C, Ridzon DA, Broomer AJ, Zhou Z, Lee DH, Nguyen JT, Barbisin M, Xu NL, Mahuvakar VR, Andersen MR, Lao KQ, Livak KJ, Guegler KJ.** 2005. Real-time quantification of microRNAs by stem-loop RT-PCR. Nucleic Acids Res **33:**e179. http://dx.doi.org/10.1093/nar/gni178.
35. **Livak KJ, Schmittgen TD.** 2001. Analysis of relative gene expression data using real-time quantitative PCR and the 2(-Delta Delta C(T)) method. Methods **25:**402–408. http://dx.doi.org/10.1006/meth.2001.1262.
36. **Rehmsmeier M, Steffen P, Höchsmann M, Giegerich R.** 2004. Fast and effective prediction of microRNA/target duplexes. RNA **10:**1507–1517. http://dx.doi.org/10.1261/rna.5248604.
37. **Lewis BP, Burge CB, Bartel DP.** 2005. Conserved seed pairing, often flanked by adenosines, indicates that thousands of human genes are microRNA targets. Cell **120:**15–20. http://dx.doi.org/10.1016/j.cell.2004.12.035.
38. **Krek A, Grün D, Poy MN, Wolf R, Rosenberg L, Epstein EJ, MacMenamin P, da Piedade I, Gunsalus KC, Stoffel M, Rajewsky N.** 2005. Combinatorial microRNA target predictions. Nat Genet **37:**495–500. http://dx.doi.org/10.1038/ng1536.
39. **Miranda KC, Huynh T, Tay Y, Ang Y-S, Tam W-L, Thomson AM, Lim B, Rigoutsos I.** 2006. A pattern-based method for the identification of microRNA binding sites and their corresponding heteroduplexes. Cell **126:**1203–1217. http://dx.doi.org/10.1016/j.cell.2006.07.031.
40. **Alexiou P, Maragkakis M, Papadopoulos GL, Simmosis VA, Zhang L, Hatzigeorgiou AG.** 2010. The DIANA-mirExTra Web server: from gene expression data to microRNA function. PLoS One **5:**e9171. http://dx.doi.org/10.1371/journal.pone.0009171.
41. **Betel D, Wilson M, Gabow A, Marks DS, Sander C.** 2008. The microRNA.org resource: targets and expression. Nucleic Acids Res **36:**D149–D153.
42. **Wong N, Wang X.** 2015. miRDB: an online resource for microRNA target prediction and functional annotations. Nucleic Acids Res **43:**D146–D152. http://dx.doi.org/10.1093/nar/gku1104.
43. **Bandyopadhyay S, Mitra R.** 2009. TargetMiner: microRNA target prediction with systematic identification of tissue-specific negative examples. Bioinformatics **25:**2625–2631. http://dx.doi.org/10.1093/bioinformatics/btp503.
44. **Vergoulis T, Vlachos IS, Alexiou P, Georgakilas G, Maragkakis M, Reczko M, Gerangelos S, Koziris N, Dalamagas T, Hatzigeorgiou AG.** 2012. TarBase 6.0: capturing the exponential growth of miRNA targets with experimental support. Nucleic Acids Res **40:**D222–D229. http://dx.doi.org/10.1093/nar/gkr1161.
45. **Adams SC, Broom AK, Sammels LM, Hartnett AC, Howard MJ, Coelen RJ, Mackenzie JS, Hall RA.** 1995. Glycosylation and antigenic variation among Kunjin virus isolates. Virology **206:**49–56. http://dx.doi.org/10.1016/S0042-6822(95)80018-2.
46. **Wang GP, Bushman FD.** 2006. A statistical method for comparing viral growth curves. J Virol Methods **135:**118–123. http://dx.doi.org/10.1016/j.jviromet.2006.02.008.
47. **Schnettler E, Sterken MG, Leung JY, Metz SW, Geertsema C, Goldbach RW, Vlak JM, Kohl A, Khromykh AA, Pijlman GP.** 2012. Non-coding flavivirus RNA displays RNAi suppressor activity in insect and mammalian cells. J Virol **86:**13486–13500. http://dx.doi.org/10.1128/JVI.01104-12.
48. **Gantier MP, McCoy CE, Rusinova I, Saulep D, Wang D, Xu D, Irving AT, Behlke MA, Hertzog PJ, Mackay F, Williams BRG.** 2011. Analysis of microRNA turnover in mammalian cells following Dicer1 ablation. Nucleic Acids Res **39:**5692–5703. http://dx.doi.org/10.1093/nar/gkr148.
49. **Mullokandov G, Baccarini A, Ruzo A, Jayaprakash AD, Tung N, Israelow B, Evans MJ, Sachidanandam R, Brown BD.** 2012. High-throughput assessment of microRNA activity and function using microRNA sensor and decoy libraries. Nat Methods **9:**840–846. http://dx.doi.org/10.1038/nmeth.2078.
50. **Li Z, Cui X, Li F, Li P, Ni M, Wang S, Bo X.** 2013. Exploring the role of human miRNAs in virus-host interactions using systematic overlap analysis. Bioinformatics **29:**2375–2379. http://dx.doi.org/10.1093/bioinformatics/btt391.
51. **Saxena T, Tandon B, Sharma S, Chameettachal S, Ray P, Ray AR, Kulshreshtha R.** 2013. Combined miRNA and mRNA signature identifies key molecular players and pathways involved in chikungunya virus infection in human cells. PLoS One **8:**e79886. http://dx.doi.org/10.1371/journal.pone.0079886.
52. **Sedano CD, Sarnow P.** 2014. Hepatitis C virus subverts liver-specific miR-122 to protect the viral genome from exoribonuclease Xrn2. Cell Host Microbe **16:**257–264. http://dx.doi.org/10.1016/j.chom.2014.07.006.

53. **Forster F, Paster W, Supper V, Schatzlmaier P, Sunzenauer S, Ostler N, Saliba A, Eckerstorfer P, Britzen-Laurent N, Schütz G, Schmid JA, Zlabinger GJ, Naschberger E, Stürzl M, Stockinger H.** 2014. Guanylate binding protein 1-mediated interaction of T cell antigen receptor signaling with the cytoskeleton. J Immunol **192:**771–781. http://dx.doi.org/10.4049/jimmunol.1300377.
54. **Hussain M, Torres S, Schnettler E, Funk A, Grundhoff A, Pijlman GP, Khromykh AA, Asgari S.** 2012. West Nile virus encodes a microRNA-like small RNA in the 3′ untranslated region which up-regulates GATA4 mRNA and facilitates virus replication in mosquito cells. Nucleic Acids Res **40:**2210–2223. http://dx.doi.org/10.1093/nar/gkr848.
55. **Moon SL, Dodd BJTT, Brackney DE, Wilusz CJ, Ebel GD, Wilusz J.** 2015. Flavivirus sfRNA suppresses antiviral RNA interference in cultured cells and mosquitoes and directly interacts with the RNAi machinery. Virology **485:**322–329. http://dx.doi.org/10.1016/j.virol.2015.08.009.
56. **Molina PE, Amedee A, Lecapitaine NJ, Zabaleta J, Mohan M, Winsauer P, Vande Stouwe C.** 2011. Cannabinoid neuroimmune modulation of SIV disease. J Neuroimmune Pharmacol **6:**516–527. http://dx.doi.org/10.1007/s11481-011-9301-8.
57. **Luna JM, Scheel TKH, Danino T, Shaw KS, Mele A, Fak JJ, Nishiuchi E, Takacs CN, Catanese MT, de Jong YP, Jacobson IM, Rice CM, Darnell RB.** 2015. Hepatitis C virus RNA functionally sequesters miR-122. Cell **160:**1099–1110. http://dx.doi.org/10.1016/j.cell.2015.02.025.
58. **Cullen B.** 2013. How do viruses avoid inhibition by endogenous cellular microRNAs? PLoS Pathog **9:**e1003694. http://dx.doi.org/10.1371/journal.ppat.1003694.
59. **Bogerd HP, Skalsky RL, Kennedy EM, Furuse Y, Whisnant AW, Flores O, Schultz KLW, Putnam N, Barrows NJ, Sherry B, Scholle F, Garcia-Blanco MA, Griffin DE, Cullen BR.** 2014. Replication of many human viruses is refractory to inhibition by endogenous cellular microRNAs. J Virol **88:**8065–8076. http://dx.doi.org/10.1128/JVI.00985-14.
60. **Miehe S, Bieberstein A, Arnould I, Ihdene O, Rütten H, Strübing C.** 2010. The phospholipid-binding protein SESTD1 is a novel regulator of the transient receptor potential channels TRPC4 and TRPC5. J Biol Chem **285:**12426–12434. http://dx.doi.org/10.1074/jbc.M109.068304.
61. **Scherbik SV, Brinton MA.** 2010. Virus-induced Ca2+ influx extends survival of West Nile virus-infected cells. J Virol **84:**8721–8731. http://dx.doi.org/10.1128/JVI.00144-10.
62. **Siddharthan V, Wang H, Davies CJ, Hall JO, Morrey JD.** 2014. Inhibition of West Nile virus by calbindin-D28k. PLoS One **9:**e106535. http://dx.doi.org/10.1371/journal.pone.0106535.
63. **Jin G, Klika A, Callahan M, Faga B, Danzig J, Jiang Z, Li X, Stark GR, Harrington J, Sherf B.** 2004. Identification of a human NF-kappaB-activating protein, TAB3. Proc Natl Acad Sci U S A **101:**2028–2033. http://dx.doi.org/10.1073/pnas.0307314101.
64. **Kanayama A, Seth RB, Sun L, Ea CK, Hong M, Shaito A, Chiu YH, Deng L, Chen ZJ.** 2004. TAB2 and TAB3 activate the NF-κB pathway through binding to polyubiquitin chains. Mol Cell **15:**535–548. http://dx.doi.org/10.1016/j.molcel.2004.08.008.
65. **Roh YS, Song J, Seki E.** 2014. TAK1 regulates hepatic cell survival and carcinogenesis. J Gastroenterol **49:**185–194. http://dx.doi.org/10.1007/s00535-013-0931-x.
66. **Sanjo H, Takeda K, Tsujimura T, Ninomiya-Tsuji J, Matsumoto K, Akira S.** 2003. TAB2 is essential for prevention of apoptosis in fetal liver but not for interleukin-1 signaling. Mol Cell Biol **23:**1231–1238. http://dx.doi.org/10.1128/MCB.23.4.1231-1238.2003.
67. **Van Antwerp D, Martin S, Kafri T, Green D, Verma I.** 1996. Suppression of TNF-alpha-induced apoptosis by NF-kappaB. Science **274:**787–789. http://dx.doi.org/10.1126/science.274.5288.787.
68. **Liu R, Lin Y, Jia R, Geng Y, Liang C, Tan J, Qiao W.** 2014. HIV-1 Vpr stimulates NF-kappaB and AP-1 signaling by activating TAK1. Retrovirology **11:**45. http://dx.doi.org/10.1186/1742-4690-11-45.